Josep M. Paredes

MICROQUASARS AND AGNs AS SOURCES OF HIGH-ENERGY _-RAYS

Frontier objects in astrophysics and particle physics
Vulcano, May 21-27, 2006

OUTLINE

1. AGN as _-ray emitters

2. How many microquasars we know

3. μqs as high-energy _-ray sources:
   Theoretical point of view

4. μqs as high-energy _ -ray sources:
   Observational point of view

6. Summary

AGN are strong _-ray (E>100 MeV) emitters

- At least 40% of all EGRET sources are AGN Thomson et al. 1995, 1996
- Some more AGN are certainly present amongst the still unidentified sources
- All detected AGN are blazars
- No radio-quiet AGN has been detected so far by EGRET

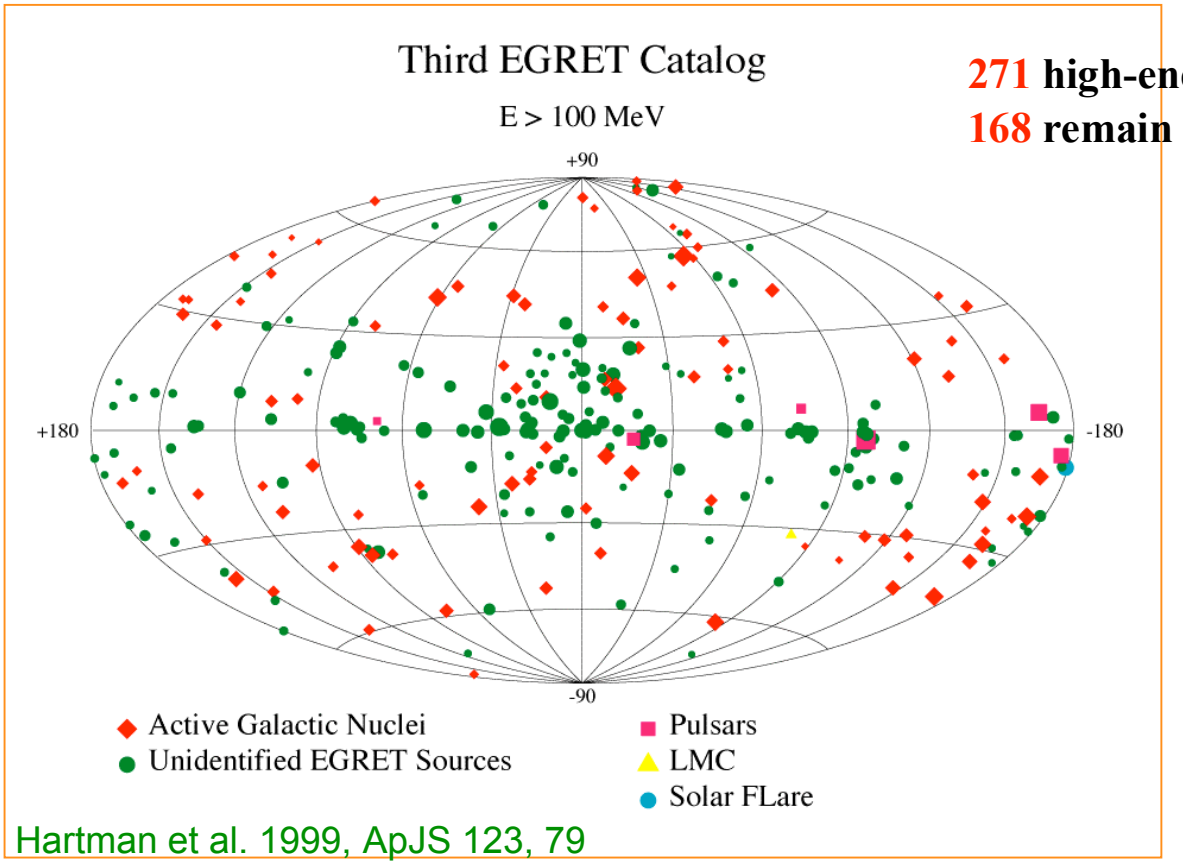

271 high-energy □-ray sources.
168 remain unidentified

72 of them in the _*b*_ < 10° area

Hartman et al. 1999, ApJS 123, 79

Why have blazars been detected by EGRET?

- High-energy particles (synchrotron emission reaches at least the infrared/optical range ➔ _-rays via IC (hadronic processes can also be important)) Padovani 1998

- Relativistic beaming (to avoid photon-photon collision and amplify the flux)
  Maraschi et al. 1992, Dondi and Ghisellini 1995

- Strong non-thermal (jet) component

Spectrum of a Quasar

Jets are the only truly broad -band sources in the universe (radio -TeV)!

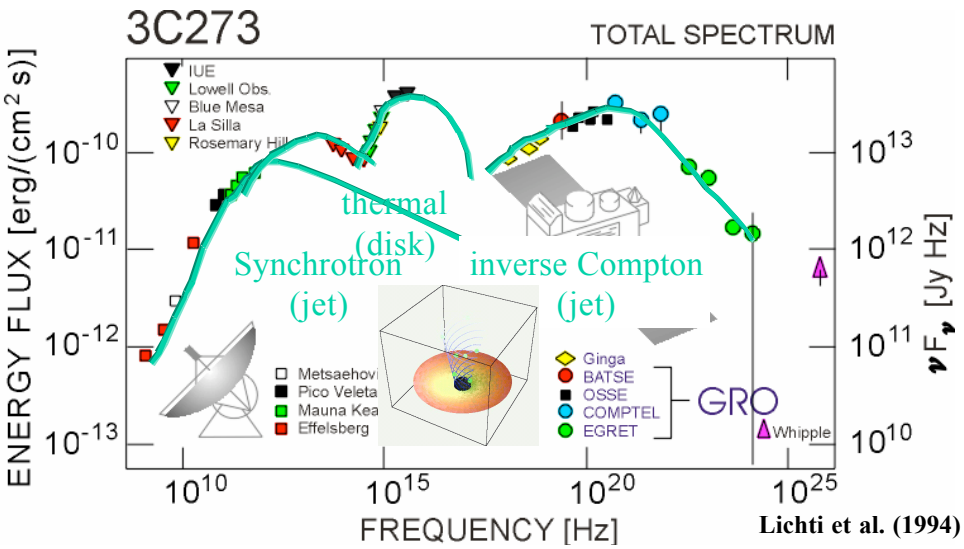

Lichti et al. (1994)

The VHE Sky – today

11 Galactic, 11 Extragalactic, GC, plus 15 unidentified

not many sources ... but at least 7 source populations !

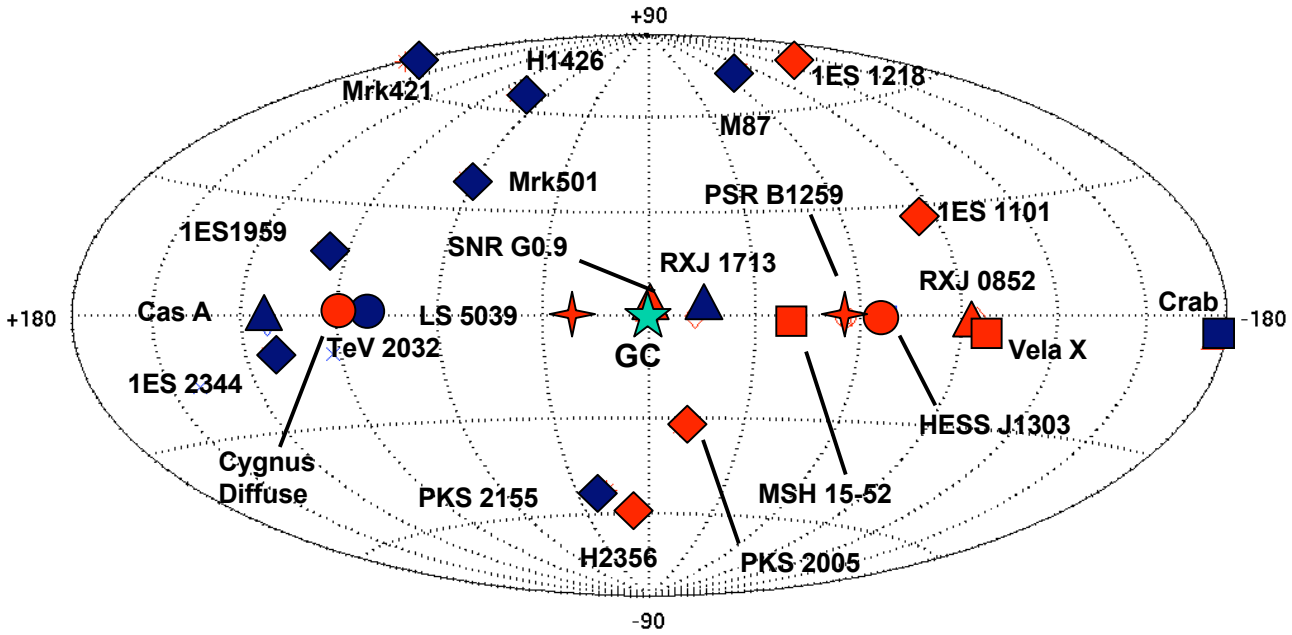

■ Pulsar Nebula ◆ AGN ✦ gal. compact

▲ SNR ● gal. unid ★ Galactic Center

PKS 2155-304

ROTSE-RXTE-HESS: simultaneous measurements

hadronic model**:** the solid line
leptonic model: the dotted line assumes a common origin for the optical and X-ray synchrotron emission
the dashed line is the case where the optical emission emanates from the VLBI core.

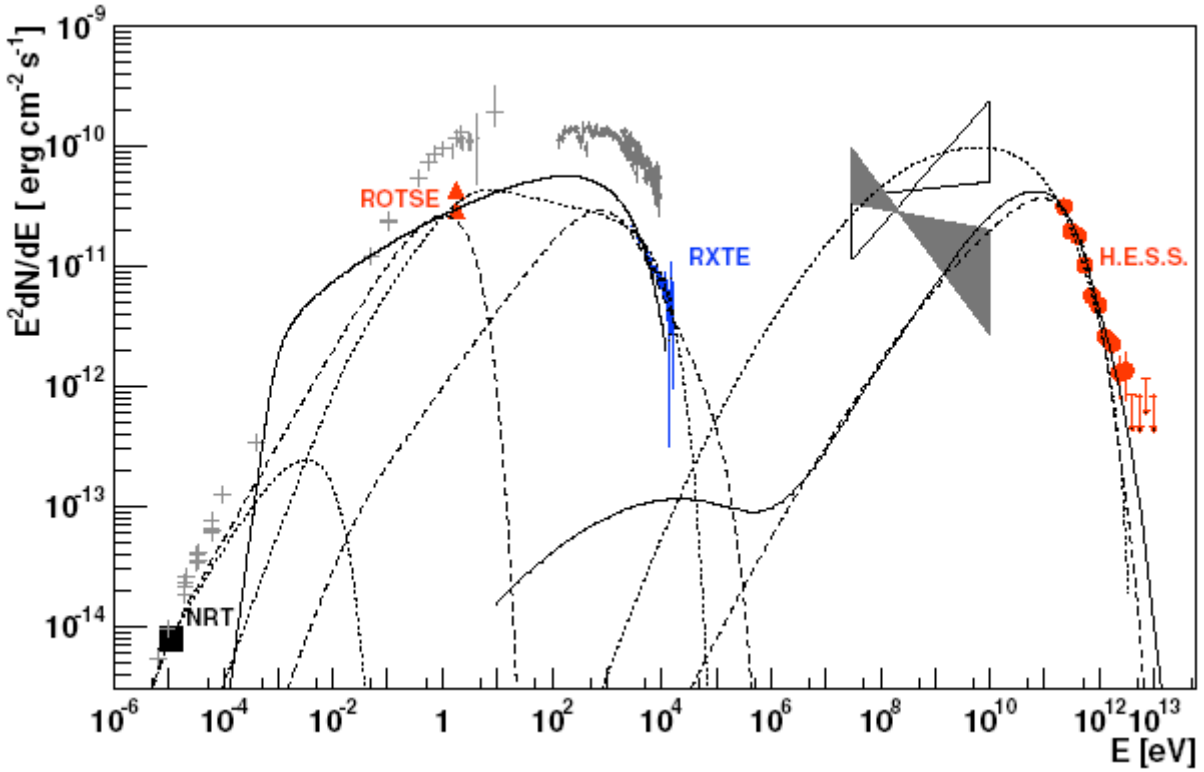

The high-energy component above 100 GeV is attenuated by interactions with the EBL and is a lower limit for the intrinsic spectrum (Primack04 model**)**.

Aharonian et al. 2005, A&A 442, 895

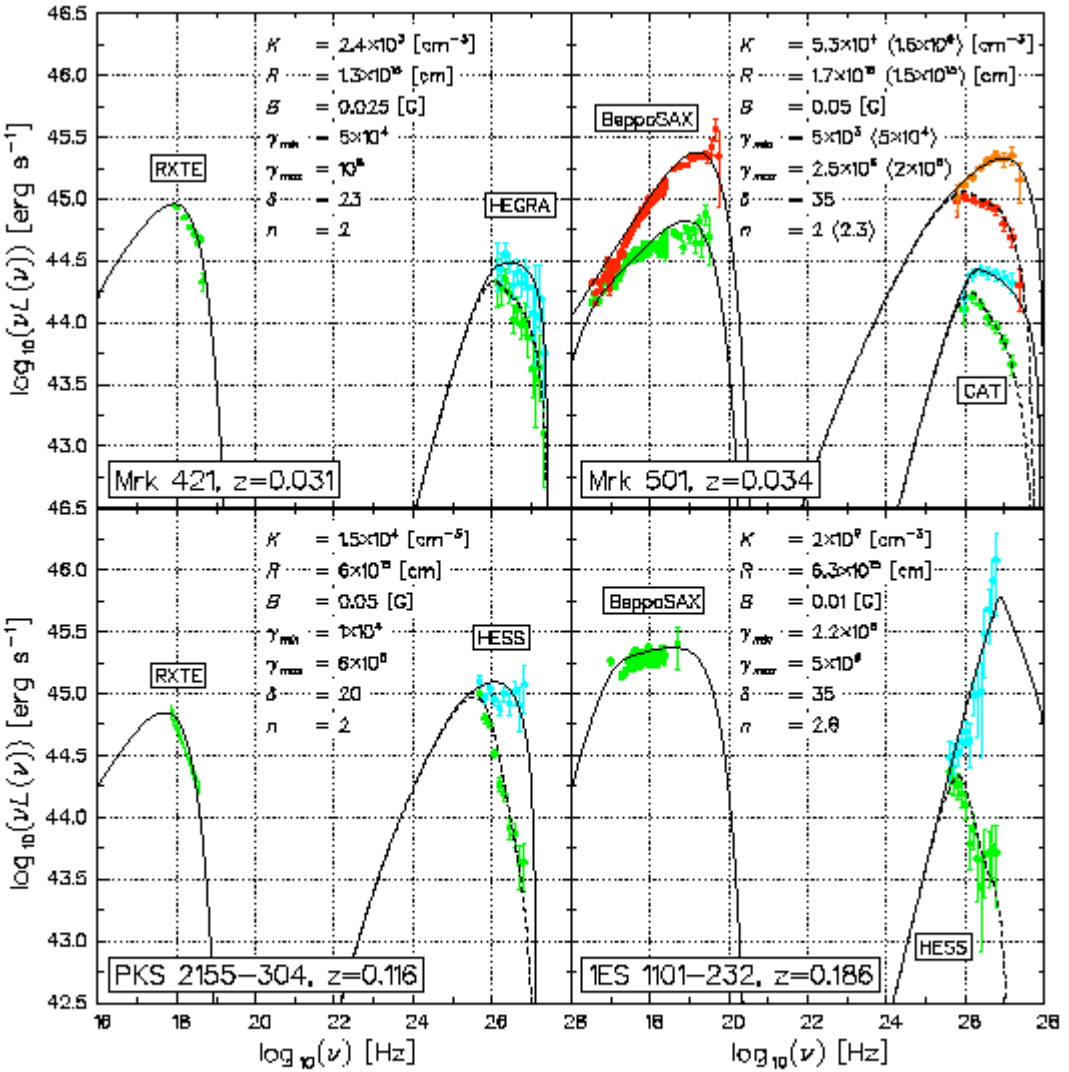

Figure 3. X-ray and TeV emission of four TeV blazars located at different redshifts. For all the sources we have applied the same SSC scenario, assuming that the emitting electrons are distributed in energy as a single power law with a low-energy cut-off at $\gamma_{\rm min}$. All the TeV spectra have been unabsorbed according to the model of Kneiske et al. (2004). Solid lines are the best fits for the expected intrinsic emission whereas dashed lines indicate the observed spectra. For an easier comparison of the different sources, we transformed the observed flux in luminosity.

Katarzynski et al. 2006, MNRAS 368, L52

X-ray binaries

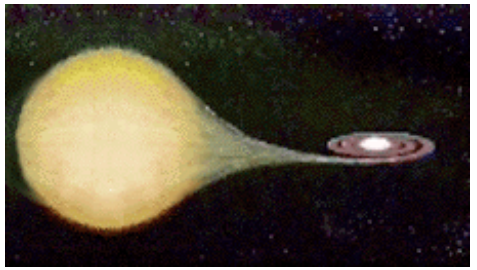

XB: A binary system containing a compact object (NS or a stellar-mass BH) accreting matter from the companion star. The accreted matter forms an accretion disc, responsible for the X-ray emission. A total of 280 XB (Liu et al. 2000, 2001).

HMXBs: (131) Optical companion with spectral type O or B. Mass transfer via decretion disc (Be stars) or via strong wind or Roche-lobe overflow.

LMXBs: (149) Optical companion with spectral type later than B. Mass transfer via Roche-lobe overflow.

Radio Emitting X-ray Binaries (REXBs) are X-ray binaries that display radio emission (synchrotron).

43 of the known 280 X-ray binaries (15%) are REXBs:
8 HMXBs and 35 LMXBs.

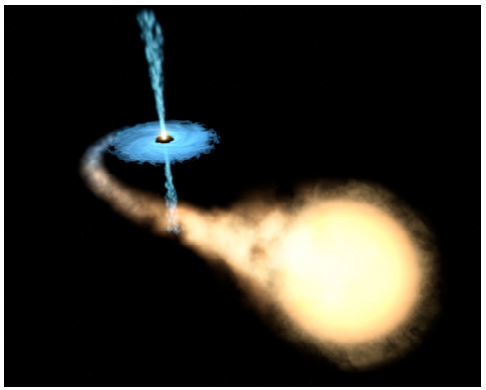

At least 15 microquasars

Maybe the majority of RXBs are microquasars (Fender 2001)

Only 10-15% of AGN are radio-loud

Kellermann et al. 1989

MICROQUASARS IN OUR GALAXY

Name	System type	D (kpc)	P_{orb} (d)	M_{comp} ($M_\odot$)	Activity radio	β_{app}	_	Jet Size (AU)	Remarks
High Mass X-ray Binaries									
LS I +61 303	B0V+NS?	2.0	26.5	-	p	≥ 0.4	-	10 - 700	**Precession ?**
V4641 Sgr	B9III+ BH	~10	2.8	**9.6**	t	≥ **9.5**	-	-	
LS 5039	O6.5V+BH?	2.6	3.9	**5.4**	p	0.18	20°	10 - 1000	
SS 433	evolved A?+BH?	4.8	13.1	11 ± 5?	p	0.26	79°	$\sim 10^4$ -10^6	**Precession**,**Hadronic**, **X-ray jet**
Cygnus X-1	O9.7I+ BH	2.5	5.6	**10.1**	p	-	40°	~ 40	
Cygnus X-3	WNe+BH?	9	0.2	-	p	0.69	73°	~ 10^4	**Radio outbursts**
Low Mass X-ray Binaries									
XTE J1118+480	K7V+BH	1.9	0.17	**6.9 ± 0.9**	t	-	-	< 0.03	??????
Circinus X-1	Subgiant+NS	~ 6.5	16.6	-	t	**> 15**	< 5°	>10^4	
XTE J1550-564	G8+BH	5.3	1.5	**9.4**	t	≥ **2**	72°	~ 10^3	**X-ray jet**
Scorpius X-1	Subgiant+NS	2.8	0.8	1.4	p	0.68	44°	~ 40	
GRO J1655-40	F5IV+BH	3.2	2.6	**7.02**	t	**1.1**	72°-85°	8000	**Precession ?**
GX 339-4	?+ BH	~ 4	1.76	**5.8 ± 0.5**	t	-	-	< 4000	
1E 1740.7-2942	?+BH ?	8.5?	12.5?	-	p	-	-	~ 10^6	
XTE J1748-288	?+BH ?	≥ 8	?	> 4.5?	t	**1.3**	-	> 10^4	
GRS 1758-258	?+ BH ?	8.5?	18.5?	-	p	-	-	~10^6	
GRS 1915+105	K-MIII+BH	12.5	33.5	**14 ± 4**	t	**1.2 -1.7**	66°-70°	~10 - 10^4	**Precession?**

Why should we expect microquasars to be _-ray emitters?

- Their extragalactic analogous, the quasars, are _-ray emitters (analogy quasar-microquasar Mirabel & Rodríguez, Nature 1992,1994)

- Theoretical models predict _-rays from microquasars, i.e.

Leptonic models: SSC Atoyan & Aharonian 1999, MNRAS 302, 253
Latham et al. 2005, AIP CP745, 323

EC Kaufman Bernadó et al. 2002, A&A 385, L10
Georganopoulos et al. 2002, A&A 388, L25

SSC+EC Bosch-Ramon et al. 2004 A&A 417, 1075

Synchrotron jet emission Markoff et al. 2003, A&A 397, 645

Hadronic models: Pion decay Romero et al. 2003, A&A 410, L1
Bosch-Ramon et al. 2005, A&A 432, 609

MQs as high-energy _ -ray sources
Theoretical point of view

Leptonic and hadronic models say that MQs are
HE _-ray sources

Leptonic high energy models

Synchrotron self Compton model

- Non-thermal flares in GRS1915+105 (Atoyan & Aharonian 1999, MNRAS 302, 253)

- Flares are caused by synchrotron radiation of relativistic electrons suffering radiative, adiabatic and energy-dependent escape losses (enables to explain the rather fast steepening of the radio spectra observed for GRS 1915+105 during strong flares) in fast-expanding plasmoids (radio clouds)
- Continuous supply or in-situ acceleration of radio electrons
- After limiting, from the radio data, the basic parameter characterizing the expanding plasmoids, the electrons may be accelerated up to TeV energies, and the fluxes of synchrotron radiation could then extend beyond the X-ray region and the fluxes of the inverse Compton (IC) gamma-rays to high and very high energies.

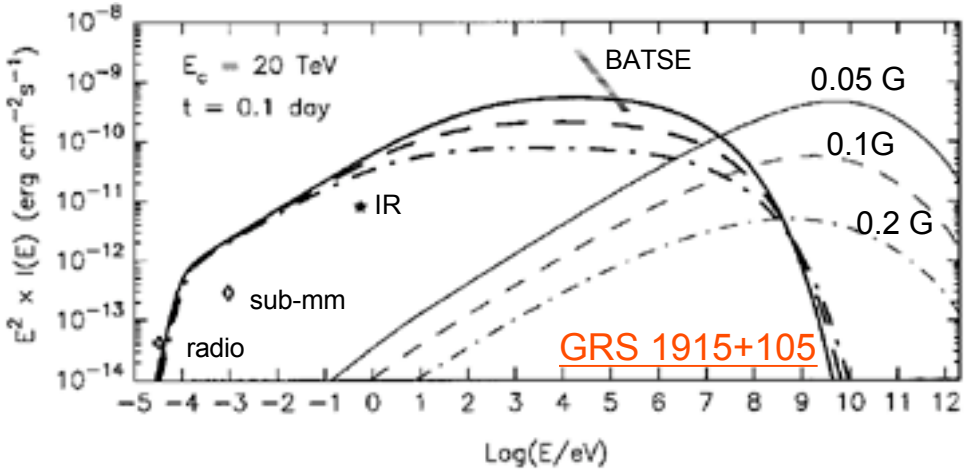

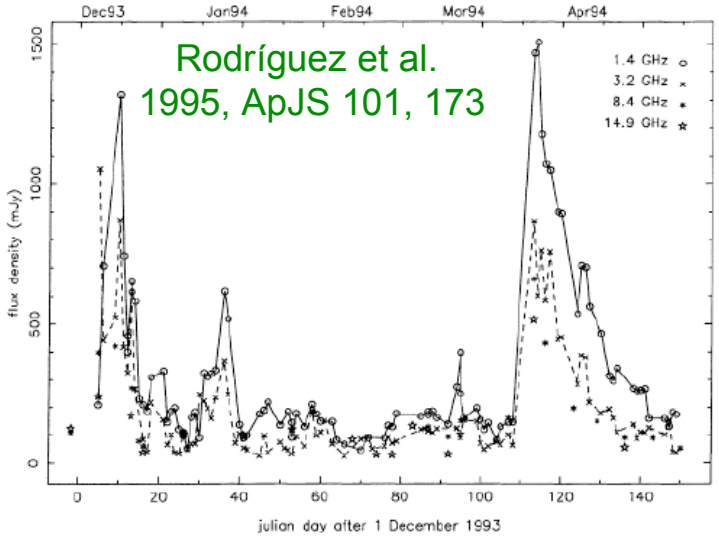

Rodríguez et al.
1995, ApJS 101, 173

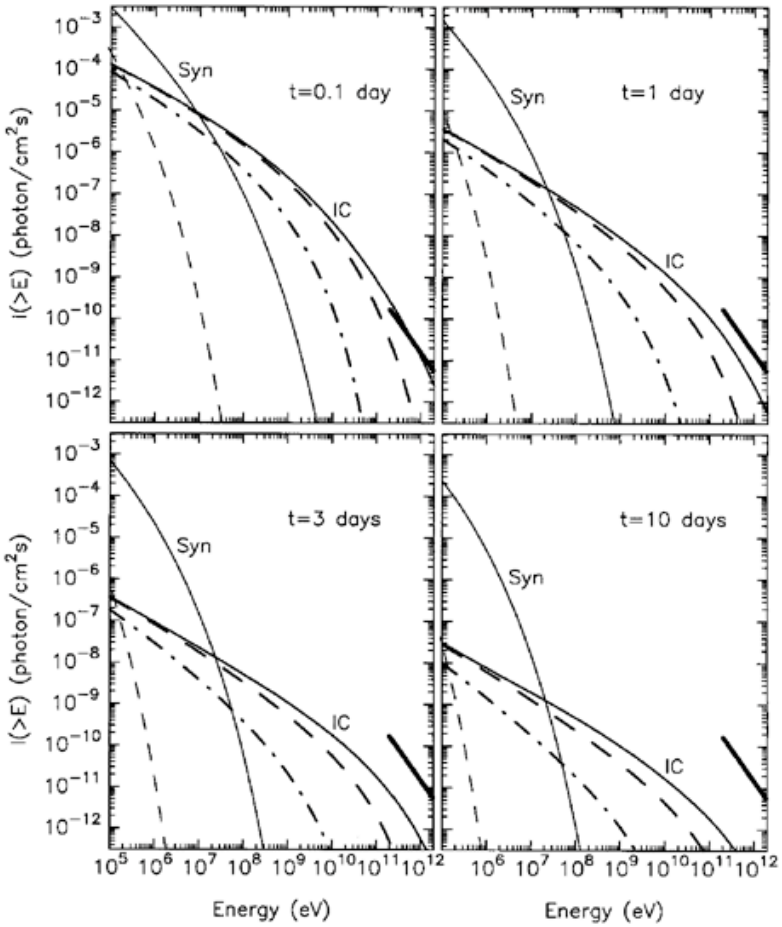

Exponential cutoff energies:

20 TeV _____

1 TeV _ _ _ _

30 GeV _ . _ . _

B = 0.05 G

IC scattering or maybe even direct synchrotron emission from the jets could dominate the high-energy emission above an MeV or so Atoyan & Aharonian 1999, MNRAS 302, 253, and 2001

External Compton Scattering - HMXB

- Jet exposed to star, disk and corona photon fields.

  Applied to Cygnus X-1 (Romero, Kaufman Bernadó & Mirabel 2002, A&A 393, L61)

- Corona (Klein-Nishina regime), disk and companion star (Thomson)
- The Compton losses in the different regions will modify the injected electron spectrum, introducing a break in the power law at the energy at which the cooling time equals the escape time.

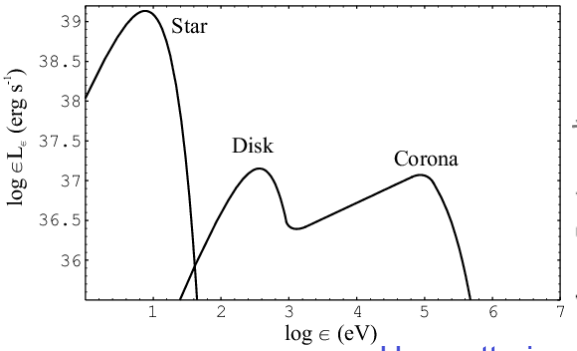

Up-scattering of
star photons (A)
disk (B)
corona (C)

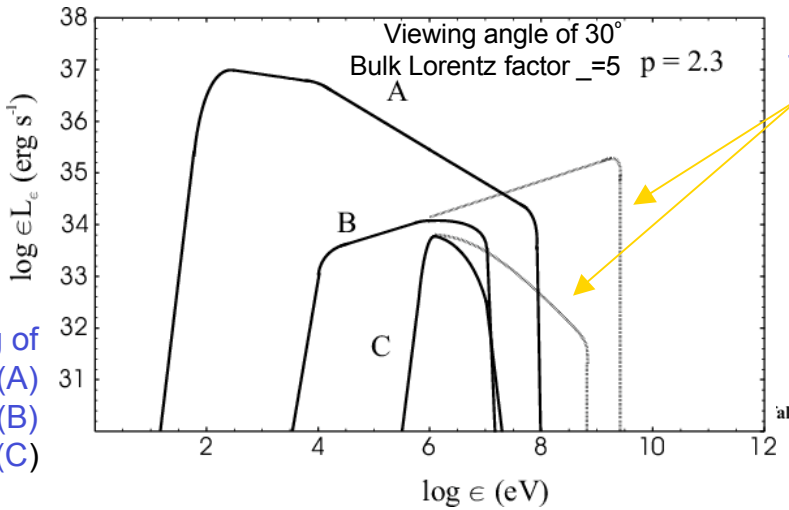

Radiation absorbed in the local field trough pair creation

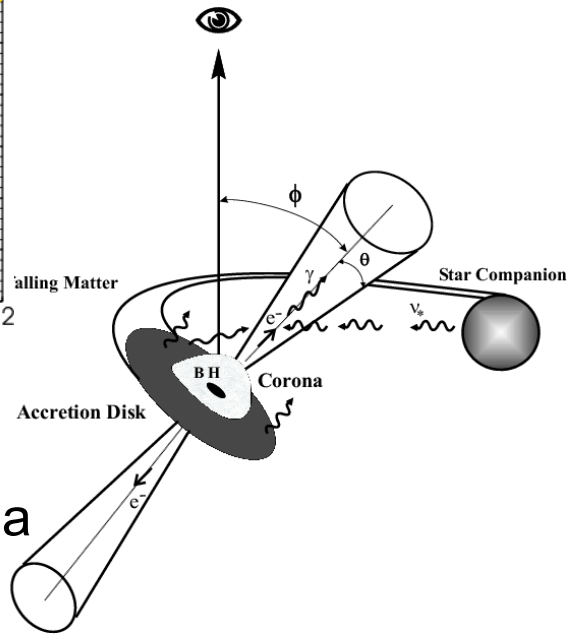

The recurrent and relatively rapid variability could be explained by the precession of the jet, which results in a variable Doppler amplification

Hadronic jet models for microquasars

- Hadronic models (only) for gamma _-ray emission:

_ Conical jet 10^{14} eV protons interacting with strong stellar wind protons, assuming efficient wind proton diffusion inside the jet.
_ Protons are injected in the base of the jet and evolve adiabaticaly.
_ Applied to explain gamma-ray emission from high mass microquasars (Romero et al. 2003, A&A 410, L1).

➢ The _-ray emission arises from the decay of neutral pions created in the inelastic collisions between relativistic protons ejected by the compact object and the ions in the stellar wind.

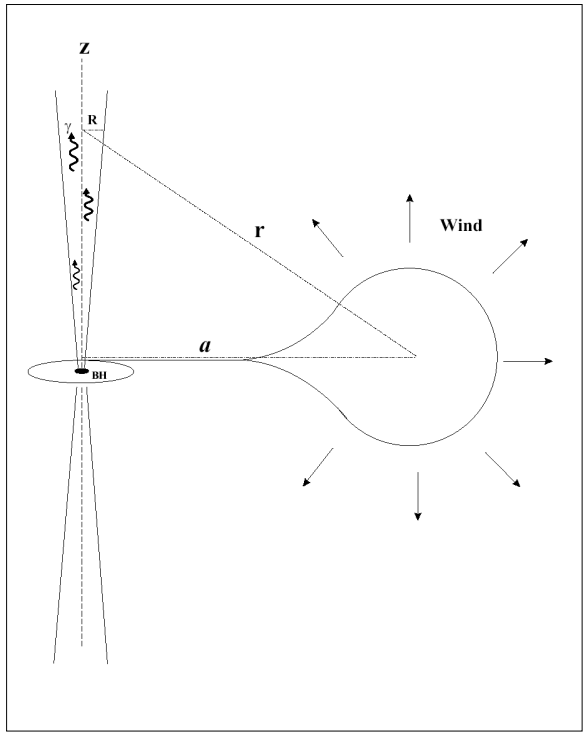

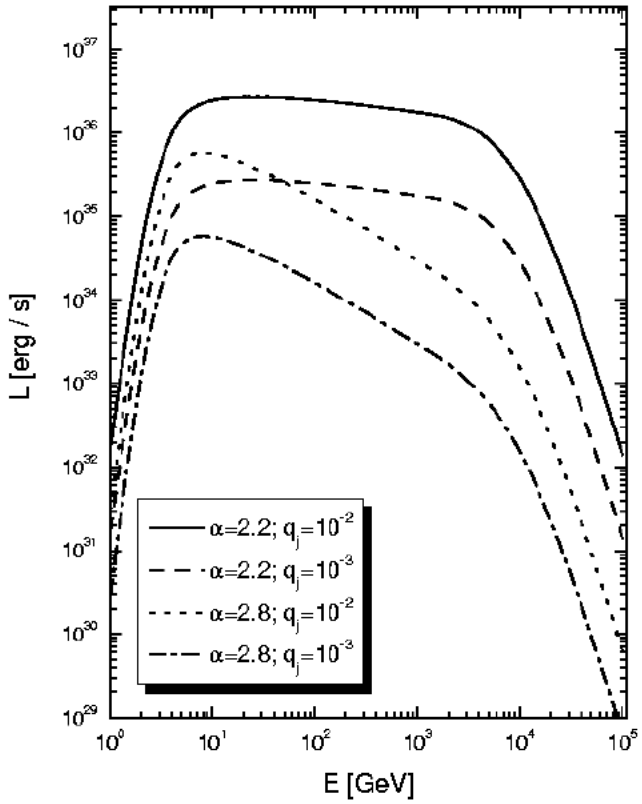

The only requisites for the model are a windy high-mass stellar companion and the presence of multi-TeV protons in the jet.

Spherically symmetric wind and circular orbit

Romero,Torres, Kaufman, Mirabel 2003, A&A 410, L1

Interactions of hadronic beams with moving clouds in the context of accreting pulsars have been previously discussed in the literature by Aharonian & Atoyan (1996, Space Sci. Rev. 75, 357).

- Models from radio to VHE:

_Released 10^{14} eV protons from the jet that diffuse through and interact with the ISM.

Computed the broadband spectrum of the emission coming out from the pp primary interactions (-rays produced by neutral pion decay) as well as the emission (synchrotron, bremsstrahlung and IC scattering) produced by the secondary particles produced by charged pion-decay.

_All the respective energy losses have been taken unto account.

_Applied to impulsive and permanent microquasar ejections.

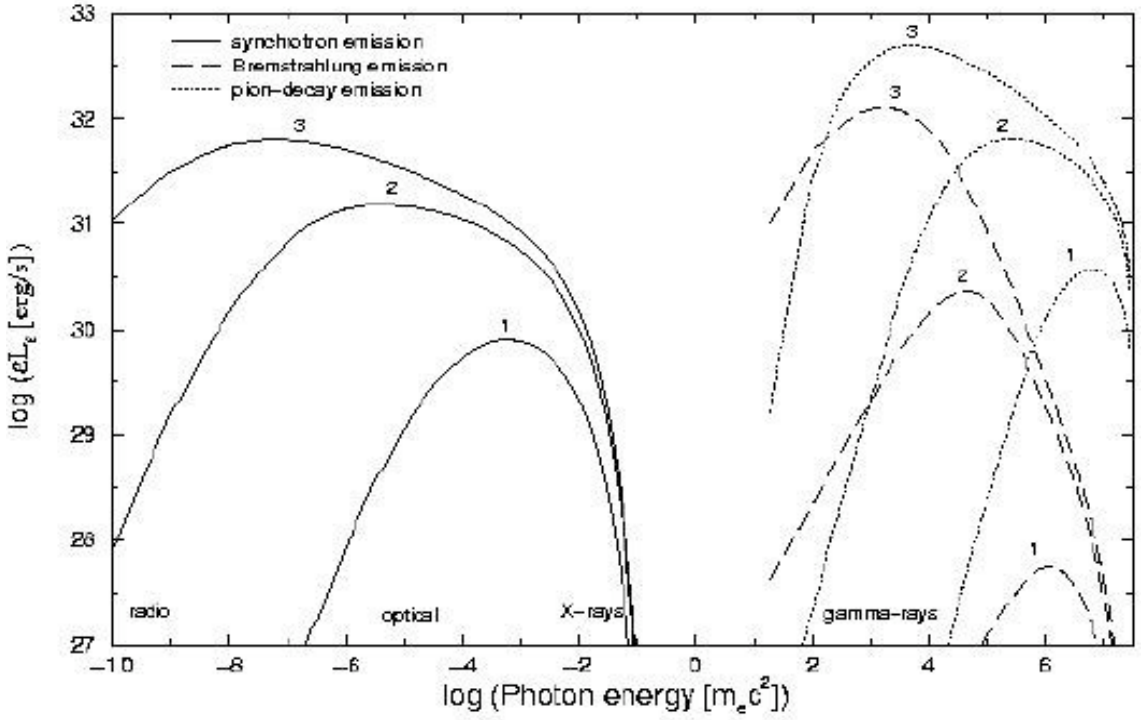

1) 100 yr
2) 1000 yr,
3) 10000 yr

$d_{MQ/cloud}$=10pc
M_{cloud}=10^5Msun
L_{jet}=10^{37} erg/s

Bosch-Ramon et al. 2005, A&A 432, 609

MQs as high-energy _ -ray sources

Observational point of view

MICROQUASARS IN OUR GALAXY High Energy Detections

Name	M_{comp} ($M_\odot$)	Radio p/t	θ_{app}	Jet Size (AU)	Note	INTEGRAL 30-50 keV (significance)	INTEGRAL 40-100 keV (count/s)	BATSE 20-100 keV (significance)	BATSE 160-430 keV (mCrab)	COMPTEL 1-30 MeV	EGRET >100 MeV	Others
High Mass X-ray Binaries												
LS I +61 303		p	≥ 0.4	10 – 700	Prec ?			5.2	5.1 ± 2.1	yes?	3EGJ0241+6103	CG135+01
V4641 Sgr	**9.6**	t	≥ **9.5**									
LS 5039	**5.4**	p	0.18	10 – 1000	Prec ?			10.7	3.7 ± 1.8	yes?	3EGJ1824 – 1514	
SS 433	11±5?	p	0.26	$\sim 10^4$ – 10^6	Prec.	13.5	<1.02	21.7	0.0 ± 2.8			
					Hadronic, X-ray jet							
Cygnus X-1	**10.1**	p		~40		676.6	66.4 ± 0.1	1186.8	924.5 ± 2.5	yes		SIGMA
Cygnus X-3		p	0.69	$\sim 10^4$	Radio outb.	122.7	5.7 ± 0.1	197.8	15.5 ± 2.1			OSSE, TeV?
Low Mass X-ray Binaries												
Circinus X-1		t	**> 15**	$>10^4$				3.8	0.3 ± 2.6			
XTE J1550-564	**9.4**	t	≥ **2**	$\sim 10^3$	X-ray jet	8.6	0.6 ± 0.07	17.1	-2.3 ± 2.5			
Scorpius X-1	1.4	p	0.68	~40		111.6	2.3 ± 0.1	460.6	9.9 ± 2.2			
GRO J1655-40	**7.02**	t	**1.1**	8000	Prec?			40.6	23.4 ± 3.9			OSSE(200keV)
GX 339-4	**5.8** ± 0.5	t		< 4000		21.9	0.55 ± 0.03	89.0	58.0 ± 3.5			SIGMA
1E 1740.7-2942		p		$\sim 10^6$		147.3	4.32 ± 0.03	92.4	61.2 ± 3.7			SIGMA
XTE J1748-288	> 4.5?	t	**1.3**	> 10^4				-12.4				SIGMA
GRS 1758-258		p		$\sim 10^6$		135.9	3.92 ± 0.03	74.3	38.0 ± 3.0			SIGMA
GRS 1915+105	**14** ± 4	t	**1.2** – **1.7**	~10 – 10^4	Prec?	144.9	8.63 ± 0.13	208.8	33.5 ± 2.7			SIGMA, TeV?

The first IBIS/ISGRI soft gamma-ray galactic plane survey catalog (Bird et al. 2004, ApJ 607, L33)

BATSE Earth Occultation Catalog, Deep Sample Results (Harmon et al. 2004, ApJS, 154, 585)

MICROQUASARS IN OUR GALAXY High Energy Detections

Name	M_{comp} ($M_\odot$)	Radio p/t	Jet θ_{app}	Size (AU)	Note	INTEGRAL 30-50 keV (significance)	INTEGRAL 40-100 keV (count/s)	BATSE 20-100 keV (significance)	BATSE 160-430 keV (mCrab)	COMPTEL 1-30 MeV	EGRET >100 MeV	Others
High Mass X-ray Binaries												
LS I +61 303	□	p	≥ 0.4	10 □700	Prec ?	□	□	5.2	5.1 ± 2.1	yes?	3EGJ0241+6103	**MAGIC**
V4641 Sgr	**9.6**	t	≥ 9.5	□		□	□	□	□	□	□	
LS 5039	**5.4**	p	0.18	10 □1000	Prec ?	□	□	10.7	3.7 ± 1.8	yes?	3EGJ1824 □1514	**HESS**
SS 433	11±5?	p	0.26	~10^4 □10^6	Prec.	13.5	<1.02	21.7	0.0 ± 2.8	□	□	
					Hadronic, X-ray jet							
Cygnus X-1	**10.1**	p	□	~40		676.6	66.4 ± 0.1	1186.8	924.5 ± 2.5	yes	□	
Cygnus X-3	□	p	0.69	~10^4	Radio outb.	122.7	5.7 ± 0.1	197.8	15.5 ± 2.1	□	□	
Low Mass X-ray Binaries												
Circinus X-1	□	t	> 15	>10^4		□	□	3.8	0.3 ± 2.6	□	□	
XTE J1550-564	**9.4**	t	≥ 2	~10^3	X-ray jet	8.6	0.6 ± 0.07	17.1	-2.3 ± 2.5	□	□	
Scorpius X-1	1.4	p	0.68	~40		111.6	2.3 ± 0.1	460.6	9.9 ± 2.2	□	□	
GRO J1655-40	**7.02**	t	1.1	8000	Prec?	□	□	40.6	23.4 ± 3.9	□	□	
GX 339-4	**5.8** ± 0.5	t	□	< 4000		21.9	0.55 ± 0.03	89.0	58.0 ± 3.5	□	□	
1E 1740.7-2942	□	p	□	~10^6		147.3	4.32 ± 0.03	92.4	61.2 ± 3.7	□	□	
XTE J1748-288	> 4.5?	t	1.3	> 10^4		□	□	-12.4	□	□	□	
GRS 1758-258	□	p	□	~10^6		135.9	3.92 ± 0.03	74.3	38.0 ± 3.0	□	□	
GRS 1915+105	**14** ± 4	t	1.2 □1.7	~10 □10^4	Prec?	144.9	8.63 ± 0.13	208.8	33.5 ± 2.7	□	□	

The first IBIS/ISGRI soft gamma-ray galactic plane survey catalog (Bird et al. 2004, ApJ 607, L33)

BATSE Earth Occultation Catalog, Deep Sample Results (Harmon et al. 2004, ApJS, 154, 585)

Cygnus X-3

- Suggested to emit TeV _-rays
  Chadwick et al. 1985, Nature 318, 642
- Other groups have failed to detect it
  O'Flaherty et al.1992, ApJ 396, 674
- SHALON (4.20±0.70) x10^{-13} photons/cm^2/s above 0.8 TeV
  Sinitsyna et al. 2001, Nuc. Phys. B (Proc. Suppl.) 97, 219

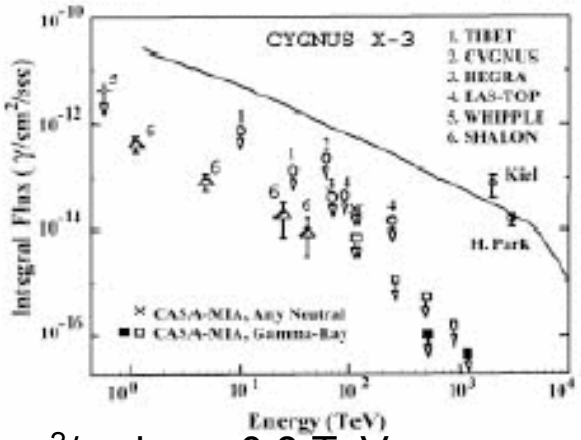

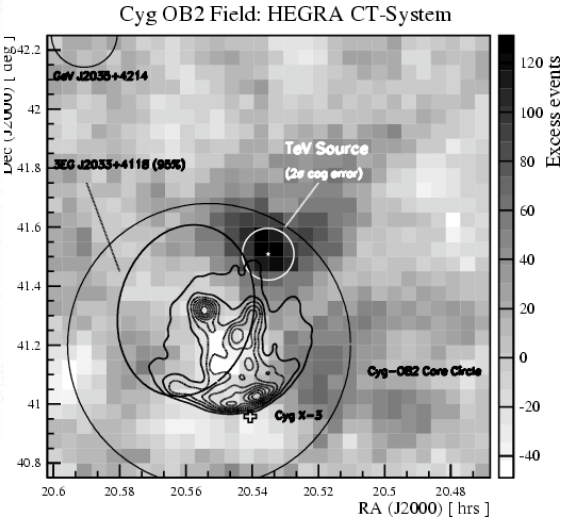

Aharonian et al. 2002, A&A 293, L37

GRS 1915+105

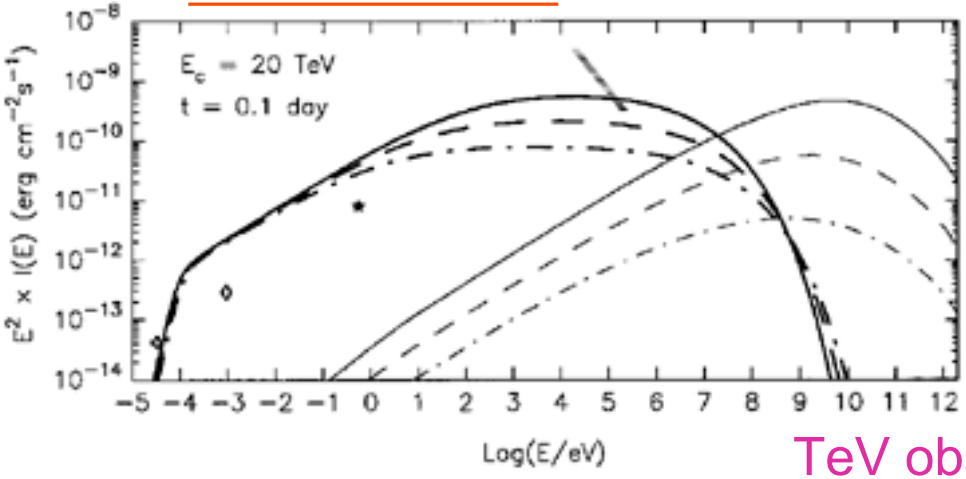

Synchrotron self Compton model

IC scattering or maybe even direct synchrotron emission from the jets could dominate the high-energy emission above an MeV or so

Atoyan & Aharonian (1999, MNRAS 302, 253)

TeV observations:

- 0.25 Crab (May-June 1996), marginal Aharonian&Heinzelmann (1998)
- 3.1sigma, marginal, Whipple (April 1998) Rovero et al. 2002, BAAA 45, 66
- (April 2003) less than 35% the flux of the Crab
  (or < 3.5x10^{-11} photons/cm^2/s) above 400 GeV Horan&Weekes (2003)

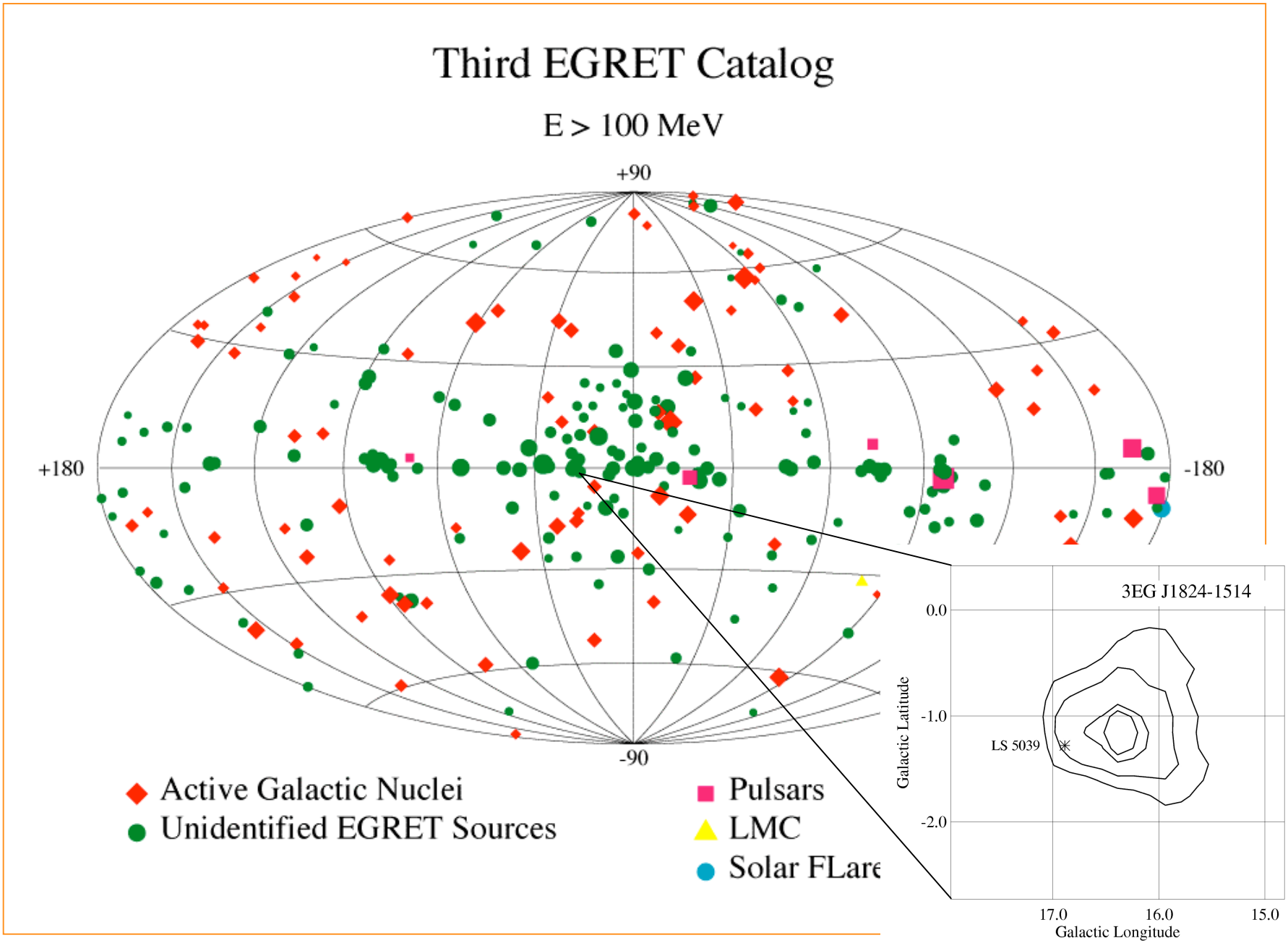

Hartman et al. 1999, ApJS 123, 79

EGRET candidate: LS 5039

Orbital phase 0.2

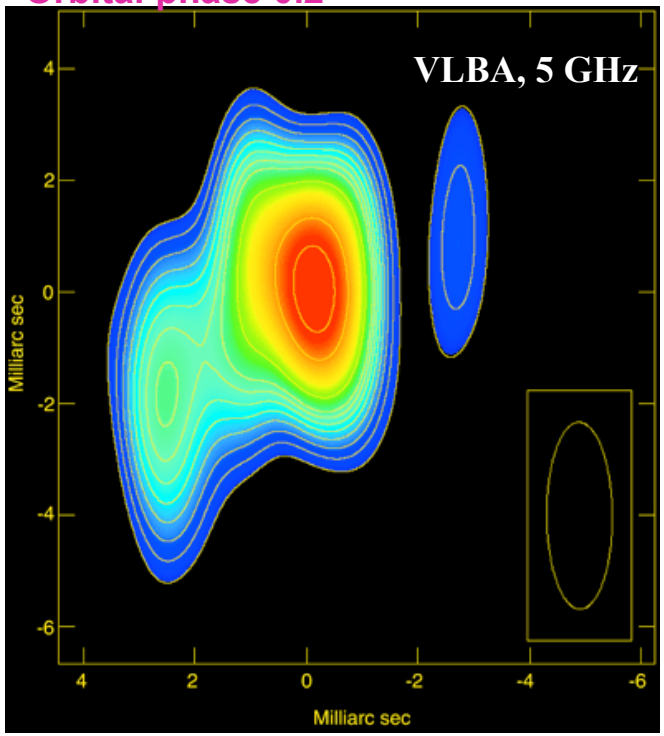

Jet parameters:

$\beta > 0.15$, $\theta < 81°$

$T_B = 9.4 \times 10^7$ K

Equipartition:

$E_e = 5 \times 10^{39}$ erg

B = 0.2 G

The photon spectral index is steeper than the $\alpha < 2$ values usually found for pulsars

Merk et al.1996, A&ASS 120, 465

L_{γ}(>100 MeV)=4×10^{35} erg·s^{-1}

LS 5039 could be related to the high energy gamma-ray source 3EG J1824-1514

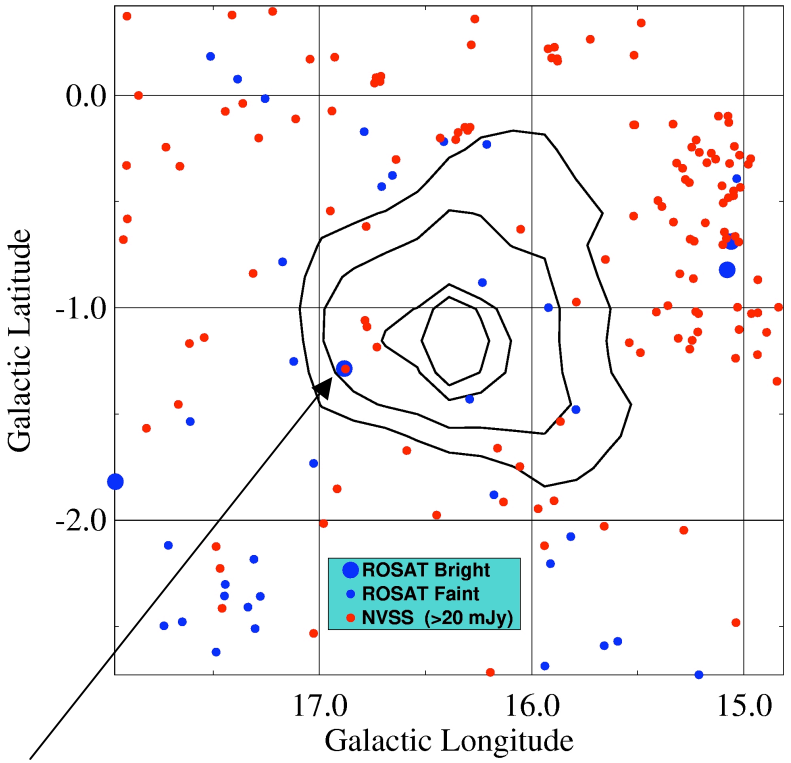

It is the only simultaneous X-ray/radio source within the 3EG J1824-1514 statistical contours.

Paredes et al. 2000, Science 288, 2340

Confirmed the **persistent nature of the jets** thanks to **EVN** and **MERLIN** observations on 2000 March 1 (Paredes et al. 2002, A&A 393, L99)

Orbital phase 0.5

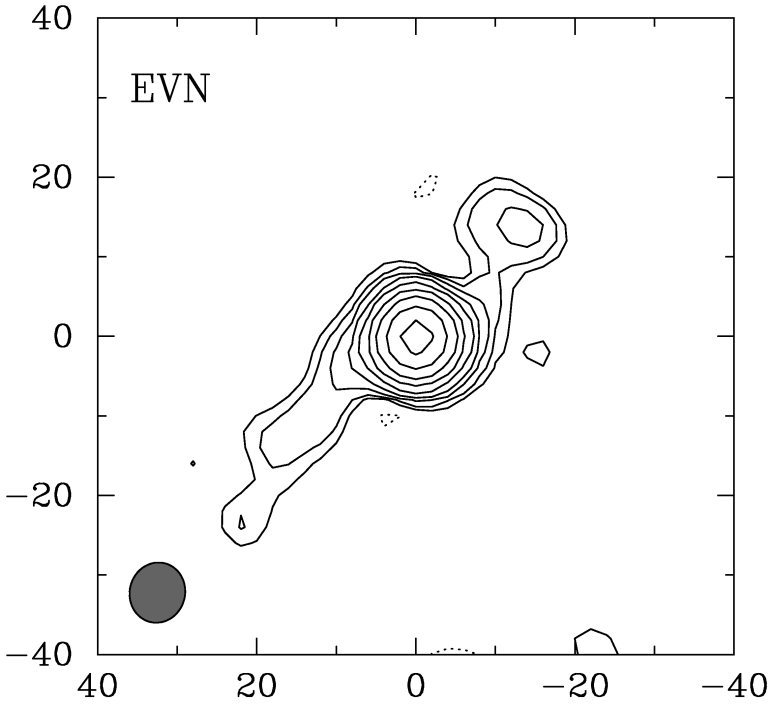

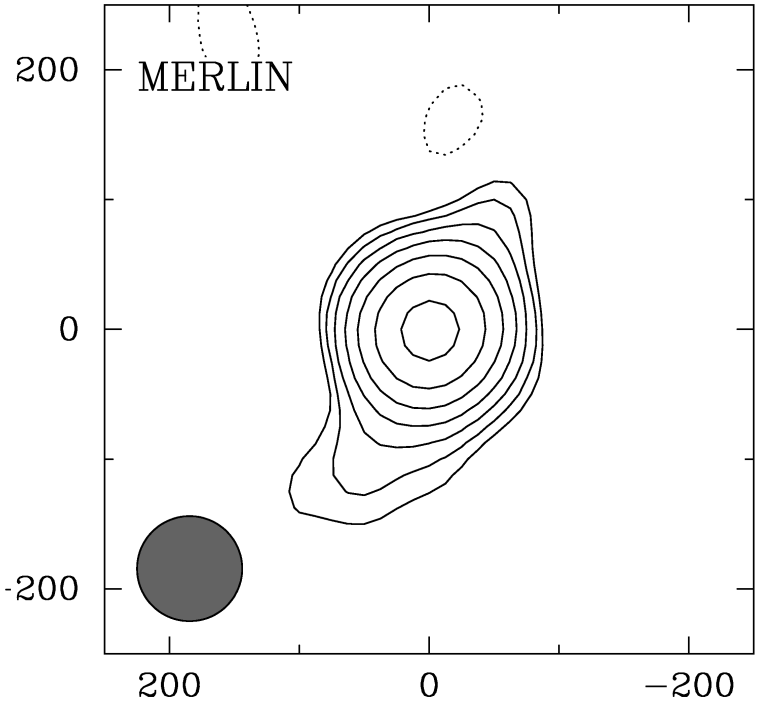

	EVN			MERLIN		
	$S_{5\,\mathrm{GHz}}$ [mJy]	Length [mas]	P.A. [°]	$S_{5\,\mathrm{GHz}}$ [mJy]	Length [mas]	P.A. [°]
Core	29.3	—	—	31.6	—	—
NW jet	2.6	24	−42	4.0	128	−29
SE jet	3.3	34	140	4.2	174	150

$$\beta \cos\theta = \frac{\mu_a - \mu_r}{\mu_a + \mu_r} = \frac{d_a - d_r}{d_a + d_r}$$

$\square > 0.17$, $\square < 80°$ 24

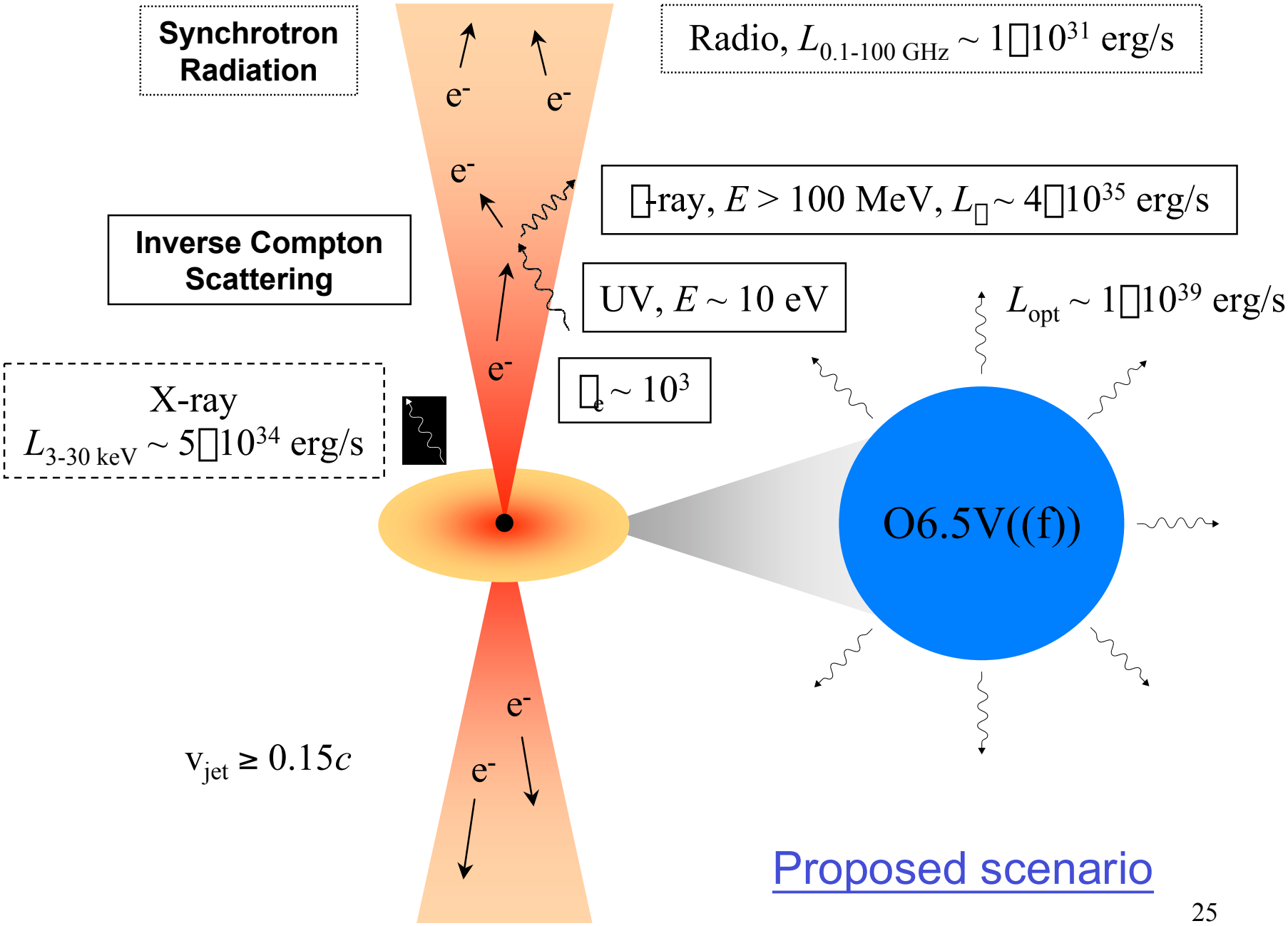

Proposed scenario

Model for the gamma-ray emission of LS 5039

Relativistic electrons entrained in a jet interacts with:

photons from the synchrotron emission of the same population of electrons (SSC)

and

photons from the star (ECS)

Synchrotron, IC and SSC losses has been taken into account.

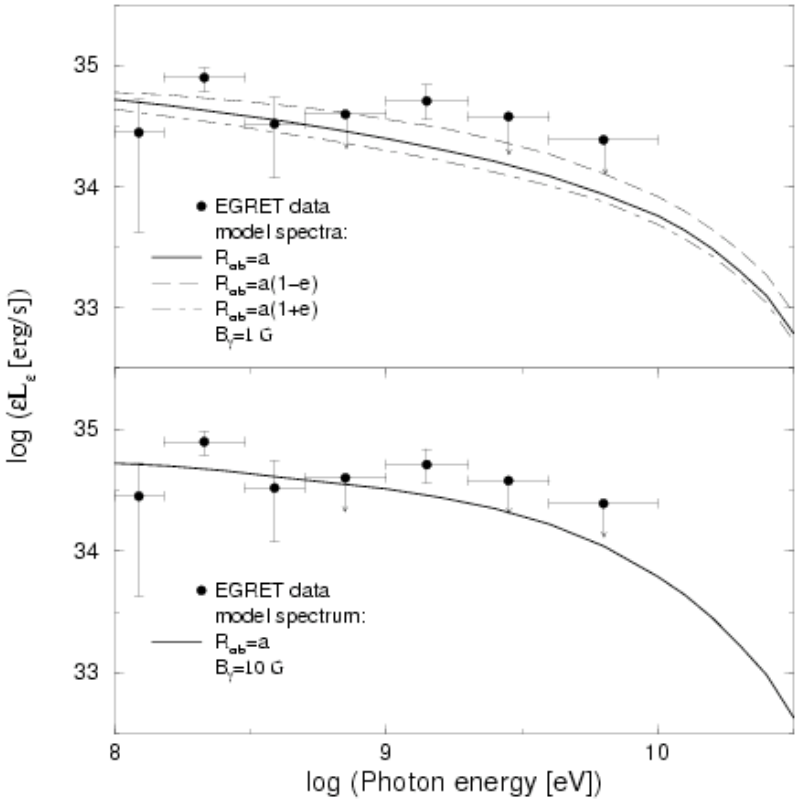

Bosch-Ramon & Paredes 2004, A&A 417, 1075

GRO J1823-12 (l/b: 17.5/-0.5)

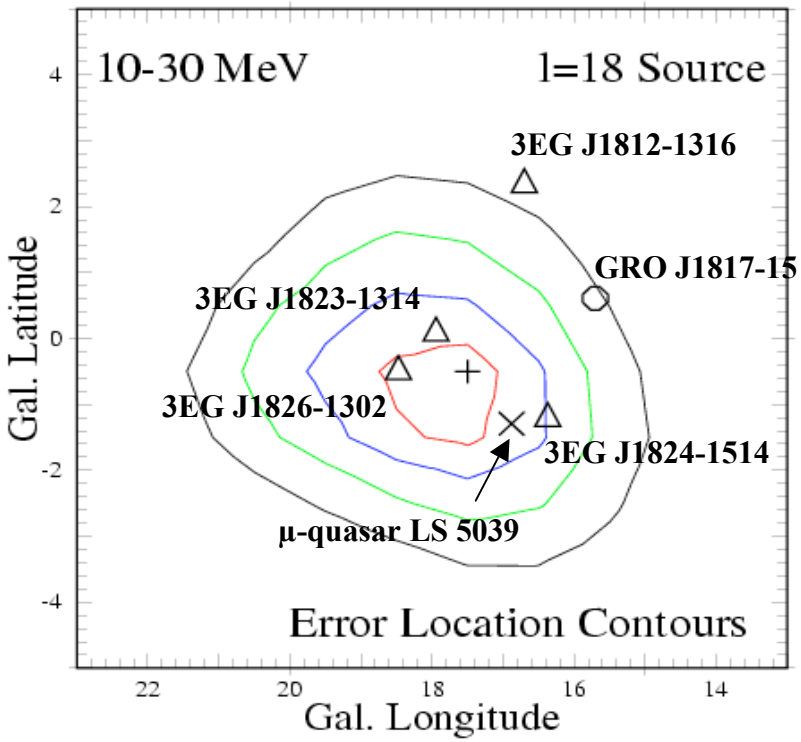

Summary

- **complicated source region**
- **possible counterparts:**
  - **3 known γ-sources (unid. EGRET)**
    (MeV emission: superposition ?)
  - **micro quasar RX J1826.2-1450/LS 5039**
    (sug. counterpart of 3EG J1824-1514;
    Paredes et al. 2000)
- **work in progress**

Collmar 2003, Proc. 4th Agile Science Workshop

A black hole in LS 5039 ?

Radial velocity curve of LS 5039

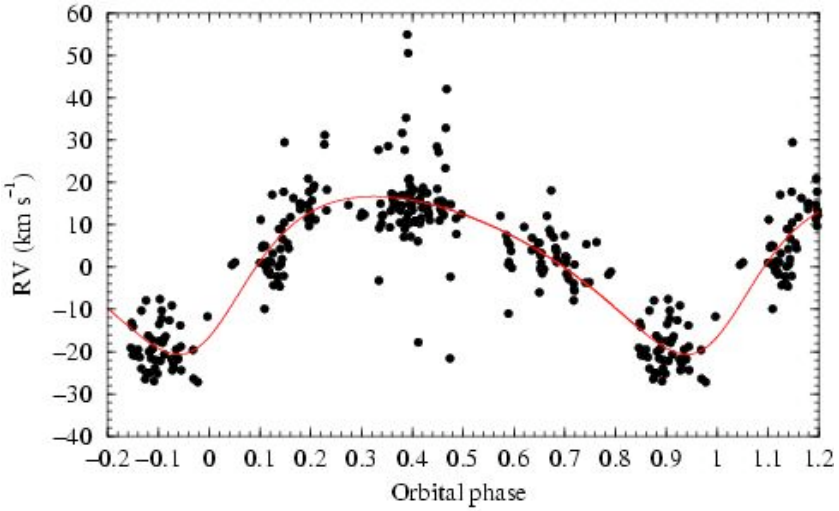

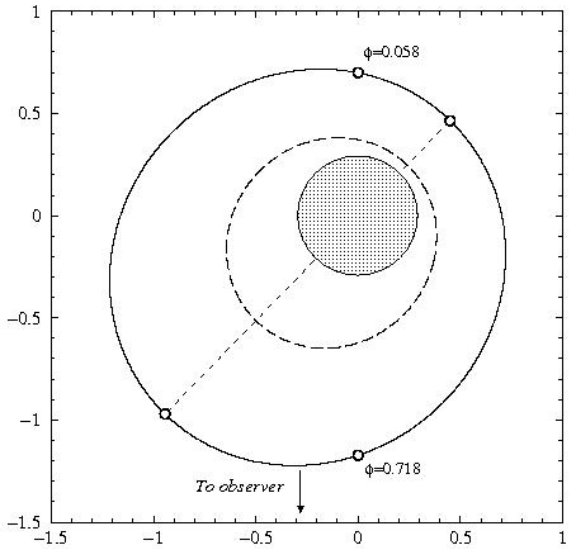

New spectroscopic observations of LS 5039
INT 2.5 m telescope (July 2002 and 2003)

New orbital ephemeris!!

P = 3.9060 ± 0.0002 d

e = 0.35 ± 0.04

Periastron at phase 0.0

And assuming pseudo-synchronisation at periastron:

i = 20.3° ± 4.0

$M_{compact}$ = 5.4 (+1.9-1.4) $M_{\odot}$

Casares et al., 2005, MNRAS, 364, 899

HESS detects LS 5039

Discovery of the TeV counterpart by HESS (Aharonian et al. 2005). Good position agreement with LS 5039. Good extrapolation of the EGRET spectrum.

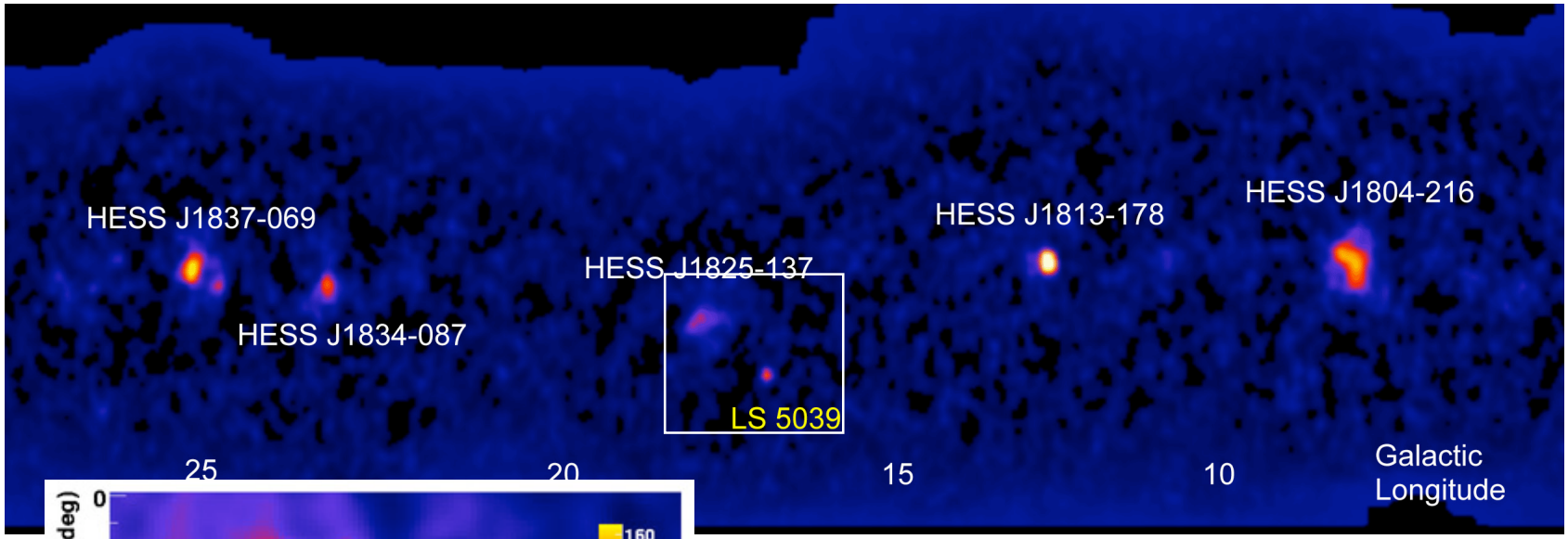

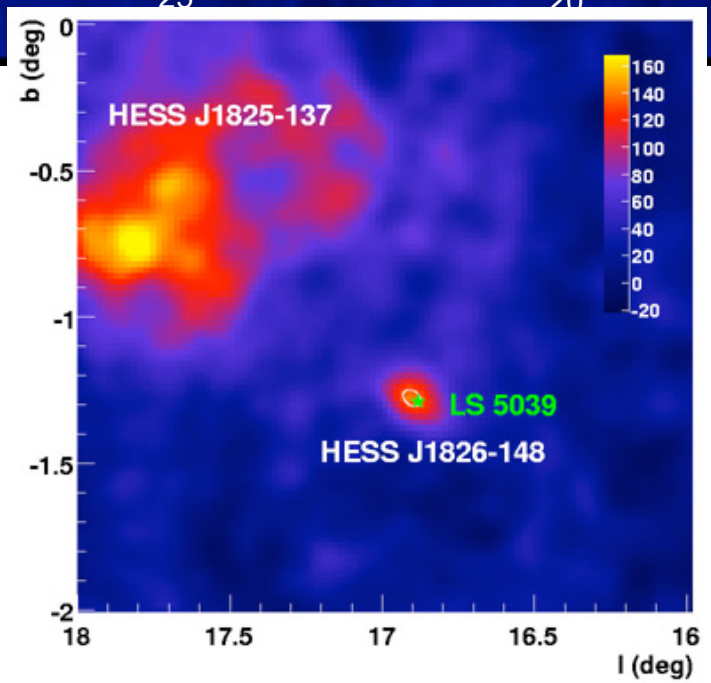

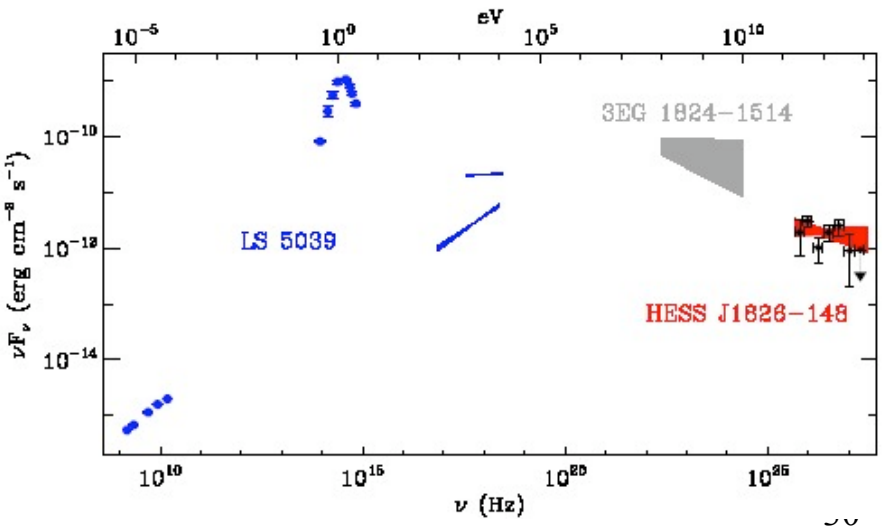

Reminder of different error box sizes.

Importance of position accuracy from TeV observations.

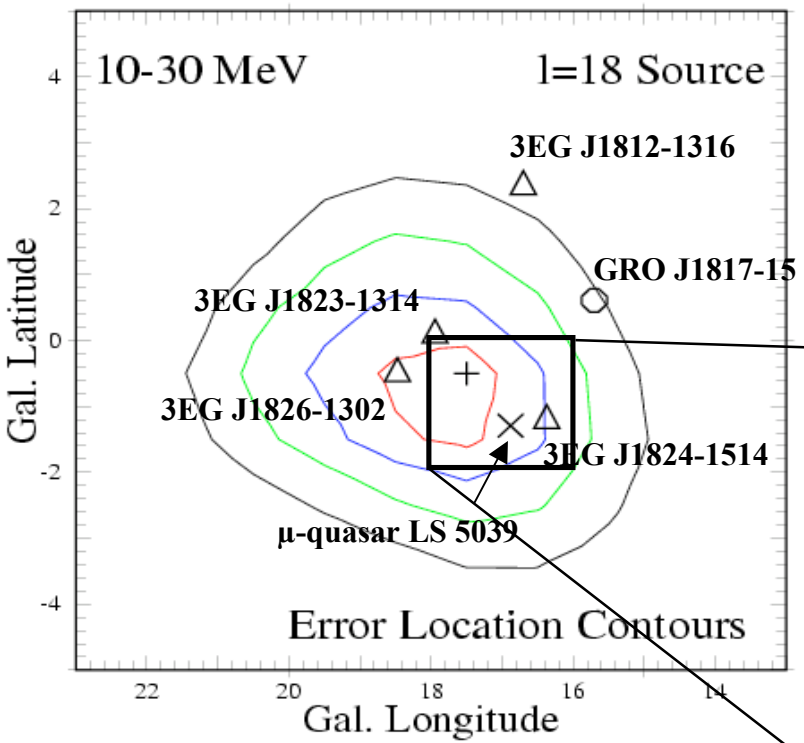

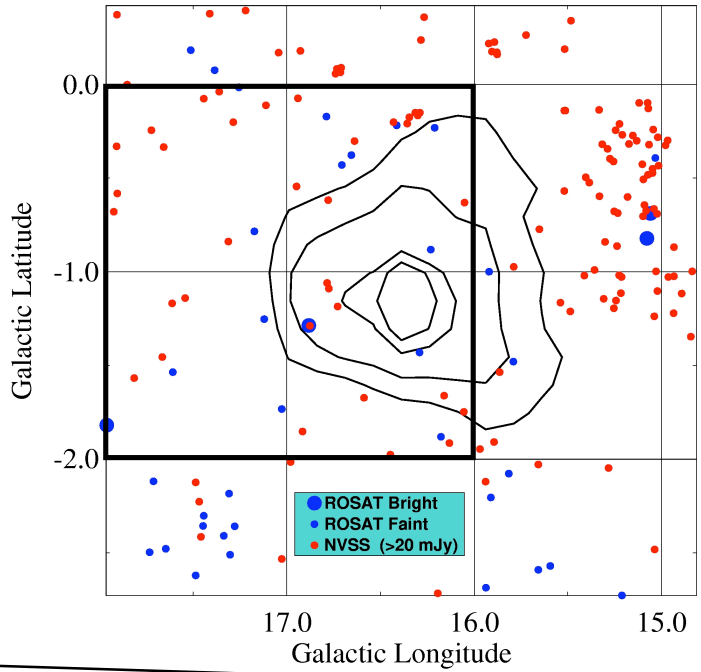

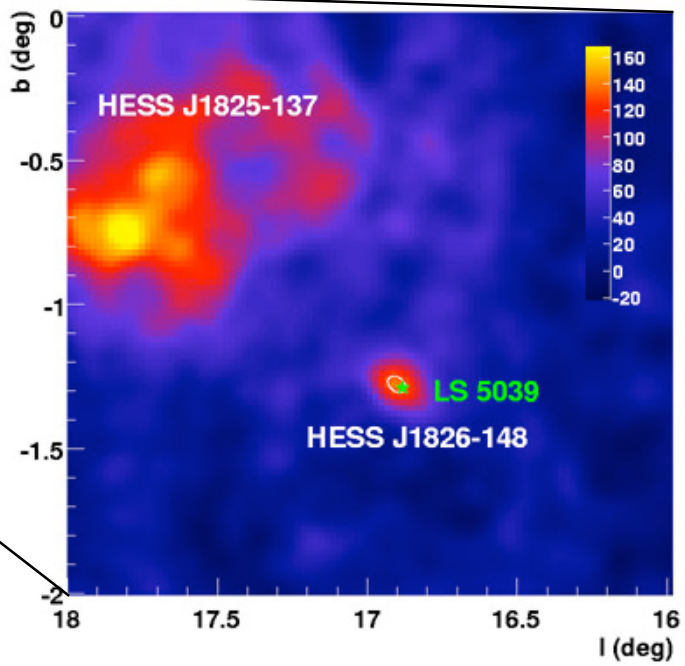

With the new orbital ephemerides (Casares et al. 2005), we have been able to see **correlated TeV and X-ray orbital variability**. Accretion/absorption.

HESS

RXTE

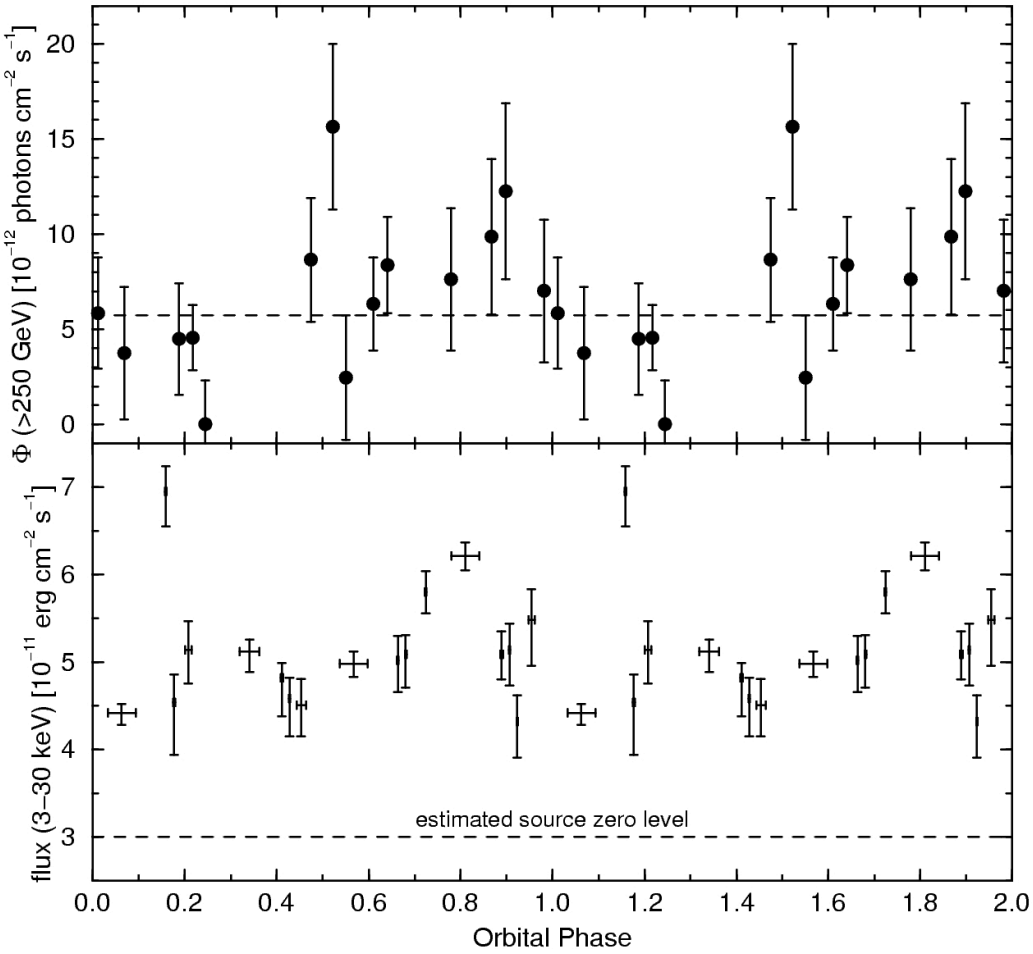

We have enough information to build up a **Spectral Energy Distribution**…

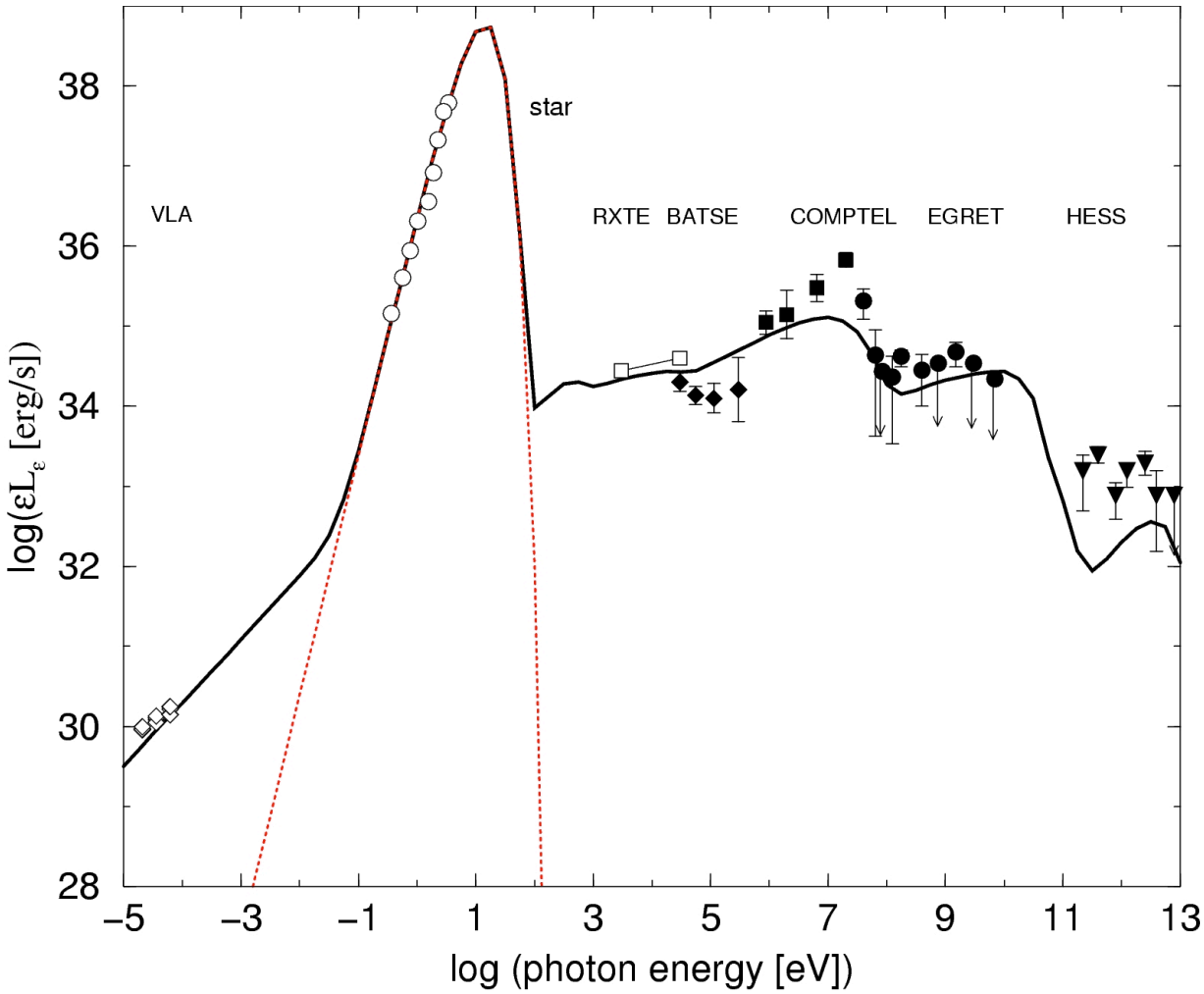

We have enough information to build up a **Spectral Energy Distribution**…

… that can be modeled to **extract physical information** (Paredes et al. 2006, A&A 451, 259).

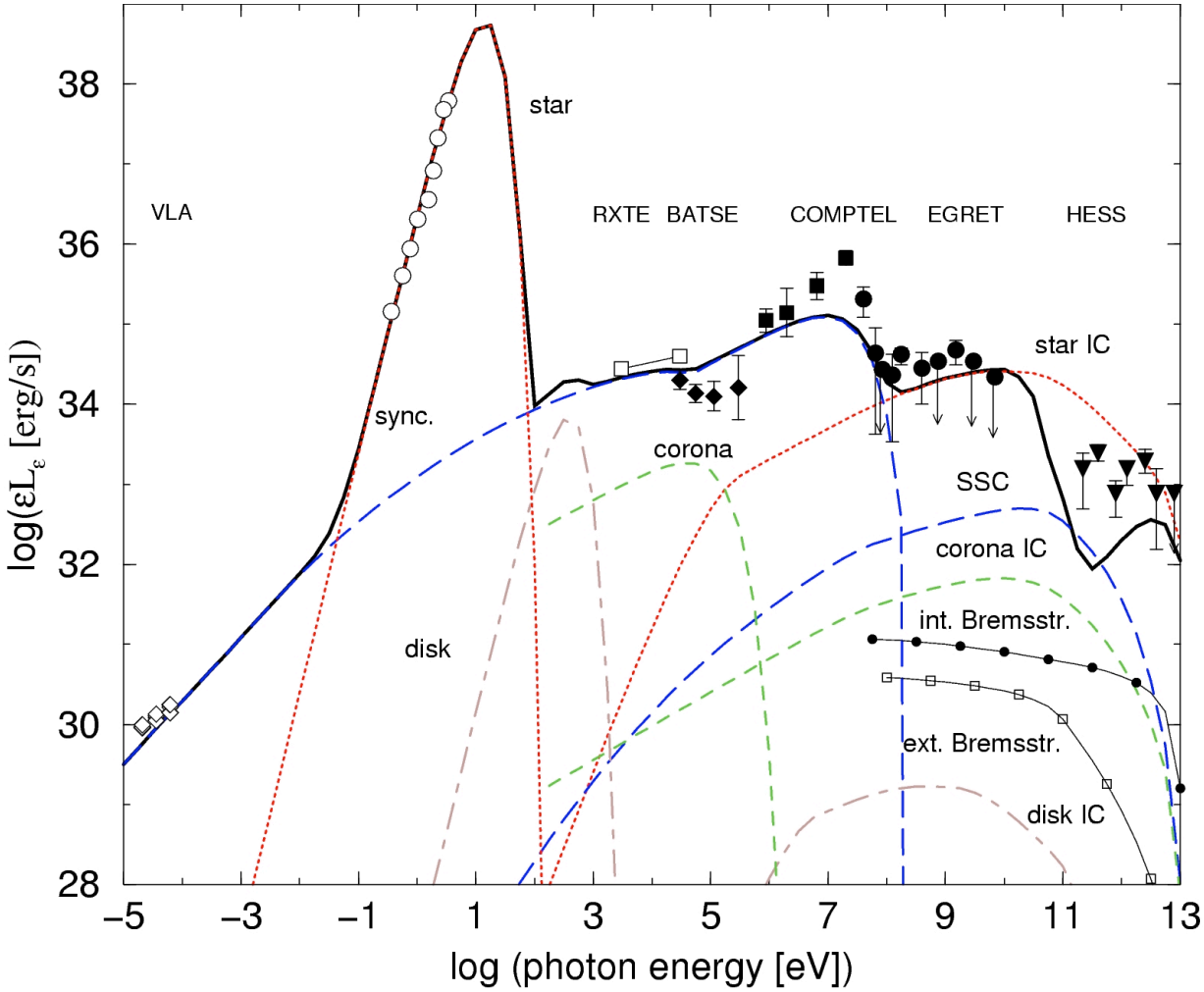

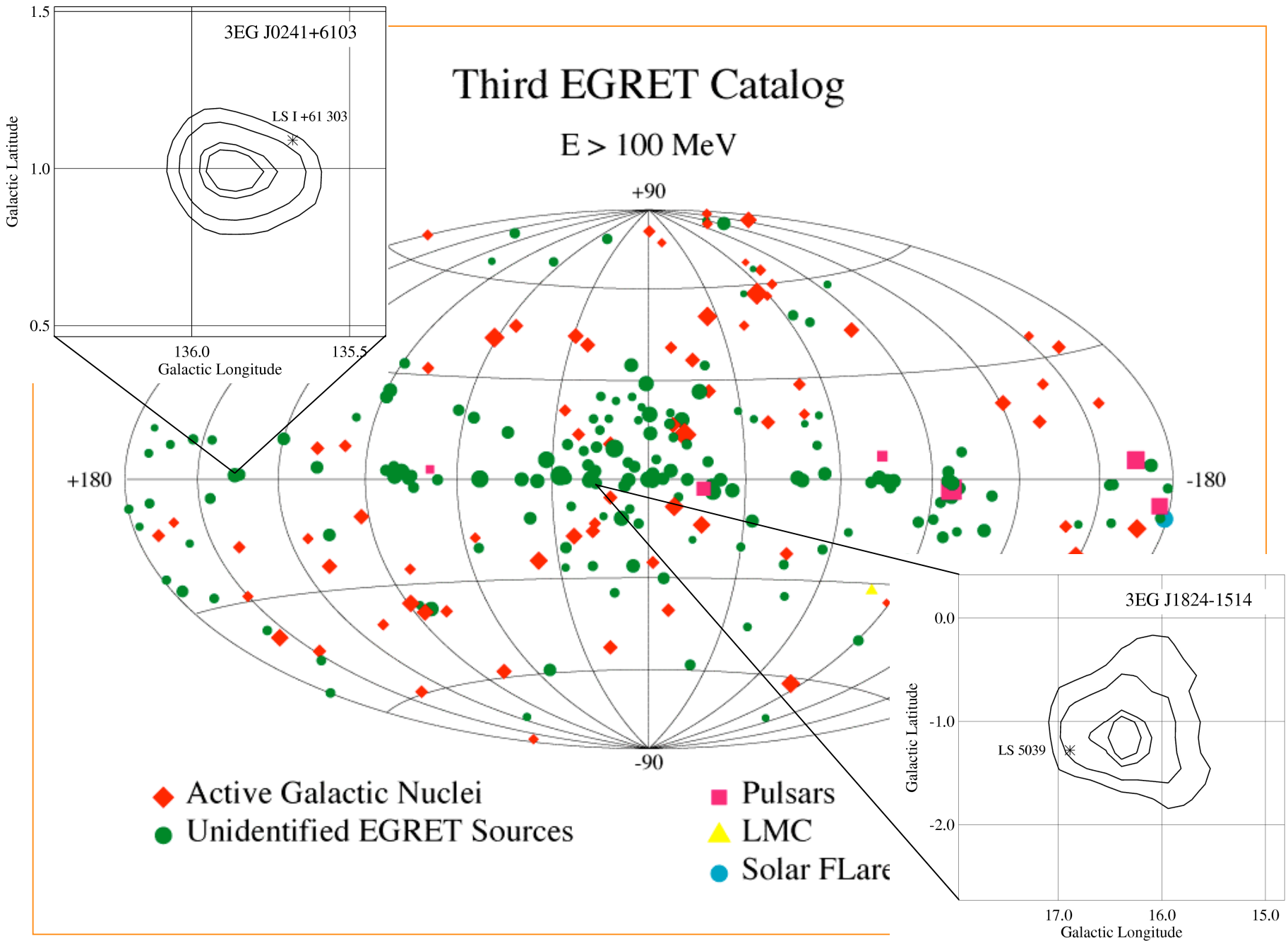

Hartman et al. 1999, ApJS 123, 79

EGRET candidate: LSI+61303

The radio emitting X-ray binary LSI+61 303, since its discovery, has been proposed to be associated with the _-ray source 2CG 135+01 (= 3EG J0241+6103)

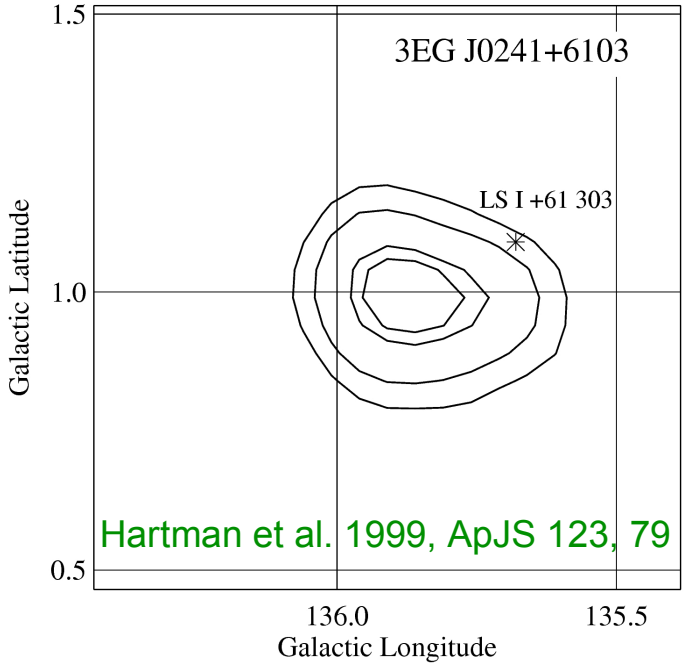

Hartman et al. 1999, ApJS 123, 79

The broadband 1 keV-100 MeV spectrum remains uncertain (OSSE and COMPTEL observations were likely dominated by the QSO 0241+622 emission)

Harrison et al. 2000, ApJ 528, 454

The EGRET angular resolution is sufficient to exclude the quasar QSO 0241+622 as the source of _-ray emission.

Strickman et al. 1998, ApJ 497, 419

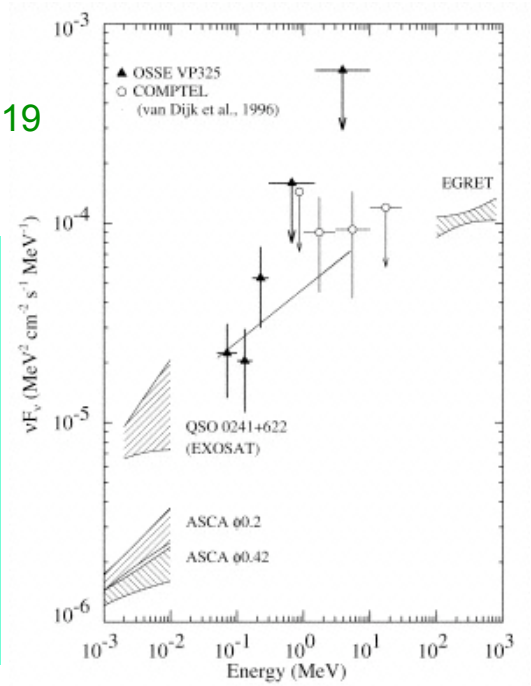

Periodic emission

Radio (P=26.496 d) _ accretion at periastron passage

Taylor&Gregory 1982, ApJ 255, 210

Optical and IR Mendelson&Mazeh 1989, MNRAS 239, 733;
Paredes et al. 1994 A&A 288, 519

X-rays Paredes et al. 1997 A&A 320, L25

_-rays ???

3EG J0241+6103 variability

Tavani et al. 1998, ApJ 497, L89

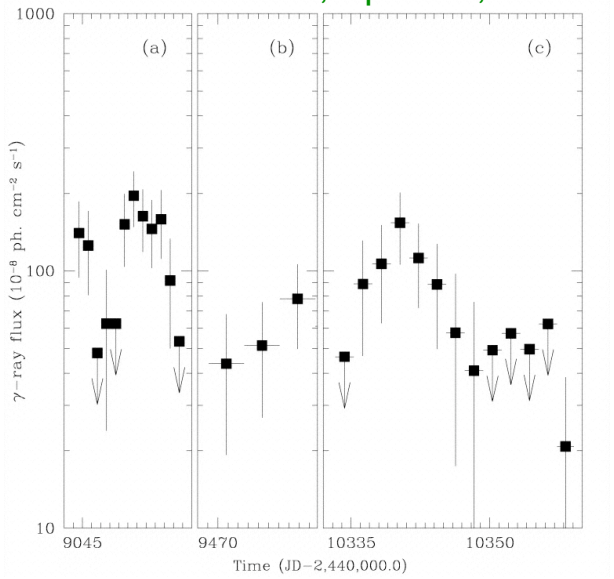

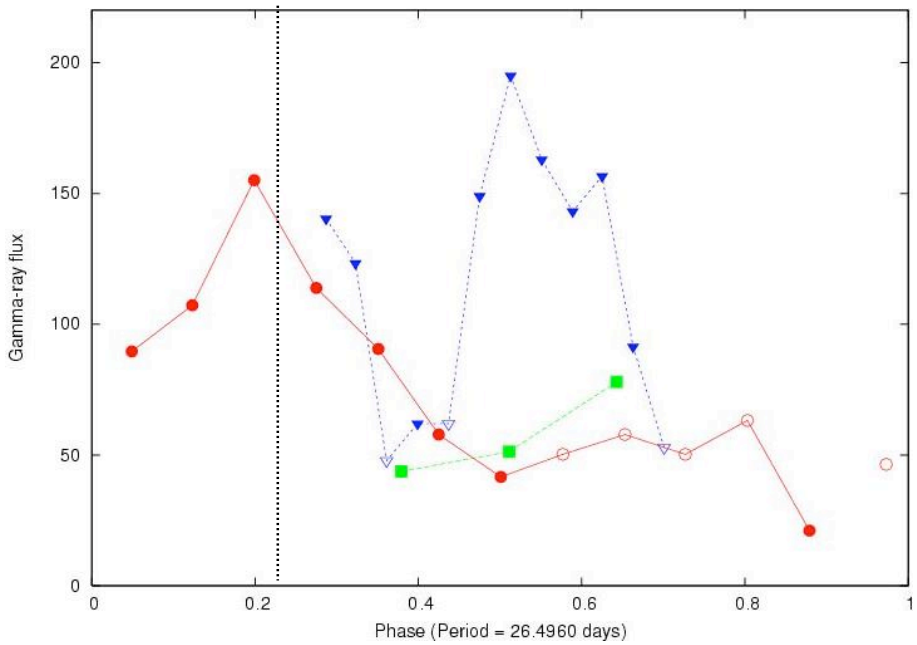

EGRET observations of 3EG J0241+6103 shows variability on short (days) and long (months) timescales

The data is consistent with an outburst at periastron passage

Massi et al. 2005 (astro-ph/0410504)

MAGIC detects LSI +61 303

MAGIC

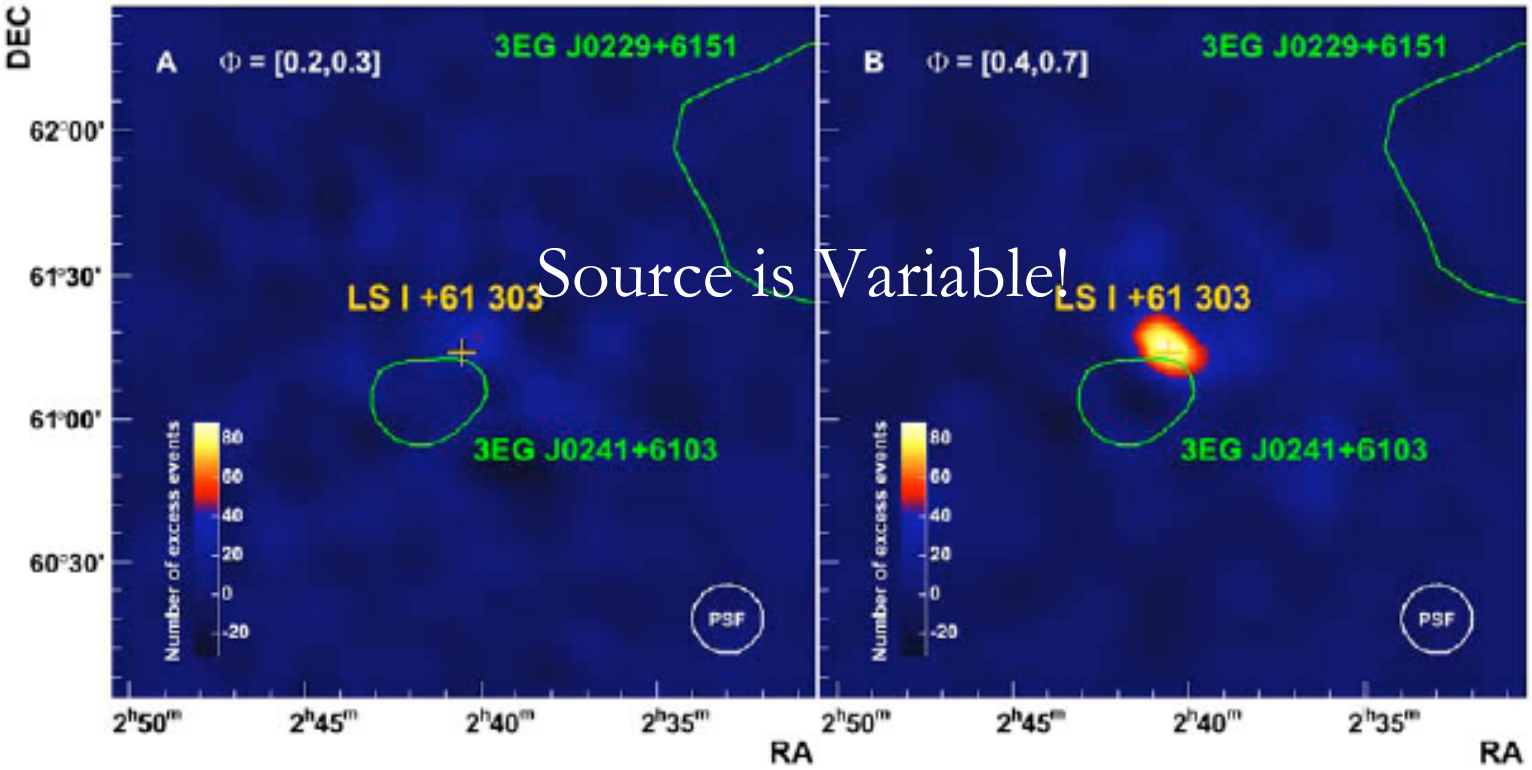

Source is Variable!

Smoothed maps of excess events above 400 GeV. (**A**) 15.5 hours corresponding to data around periastron, i.e. between orbital phases 0.2 and 0.3. (**B**) 10.7 hours at orbital phase between 0.4 and 0.7. The number of events is normalized in both cases to 10.7 hours of observation. The position of the optical source LSI +61 303 (yellow cross) and the 95% confidence level (CL) contours for 3EG J0229+6151 and 3EG J0241+6103 (green contours), are also shown. The bottom-right circle shows the size of the point spread function of MAGIC (1_ radius). No significant excess in the number of events is detected around periastron passage, while it shows up clearly (9.4_ statistical significance) at later orbital phases, in the location of LS I +61 303.

Albert et al. 2006, Science

Microquasars: LS I +61 303

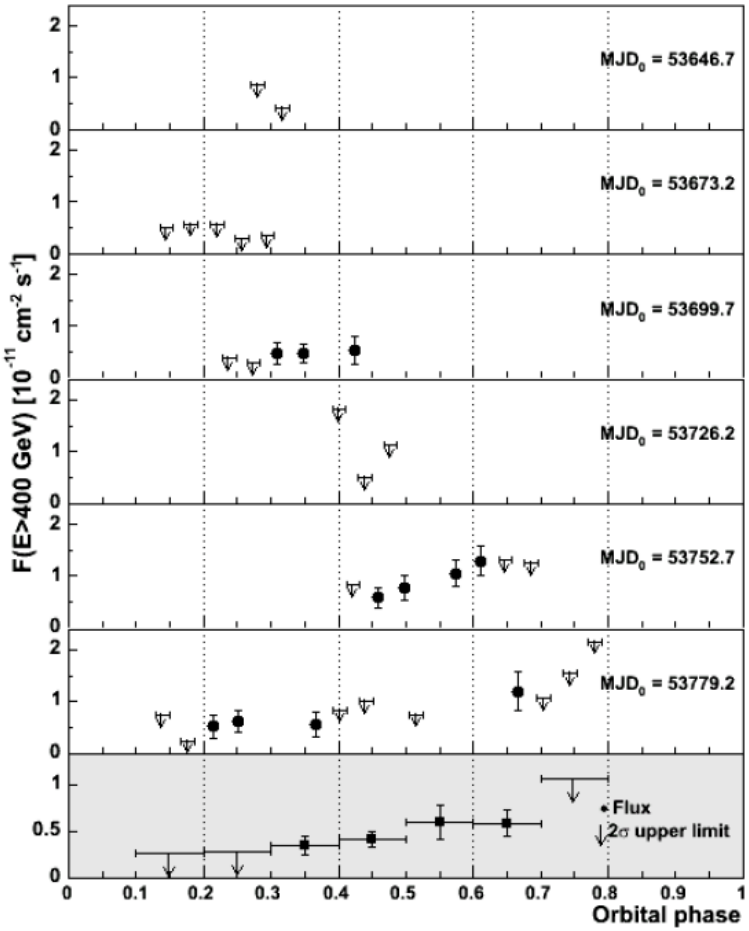

VHE flux as a function of the orbital phase for the six observed orbital cycles (6 upper panels, one point per observation night), and averaged for the entire observation time (lowermost panel).

Vertical error bars include 1_ statistical error and 10% systematic uncertainty on day-to-day relative fluxes. Only data points with more than 2_ significance are shown, and 2_ upper limits are derived for the rest. Periastron takes place at phase 0.23.

A significant increase of flux is detected from phase ~0.45 to phase ~0.65 in the 5th cycle, peaking at ~16% of the Crab Nebula flux (phase 0.61). During the following cycle, the highest flux is measured on MJD 53797 (phase 0.67).

This behavior suggests that the VHE gamma-ray emission from LSI +61 303 has a periodic nature

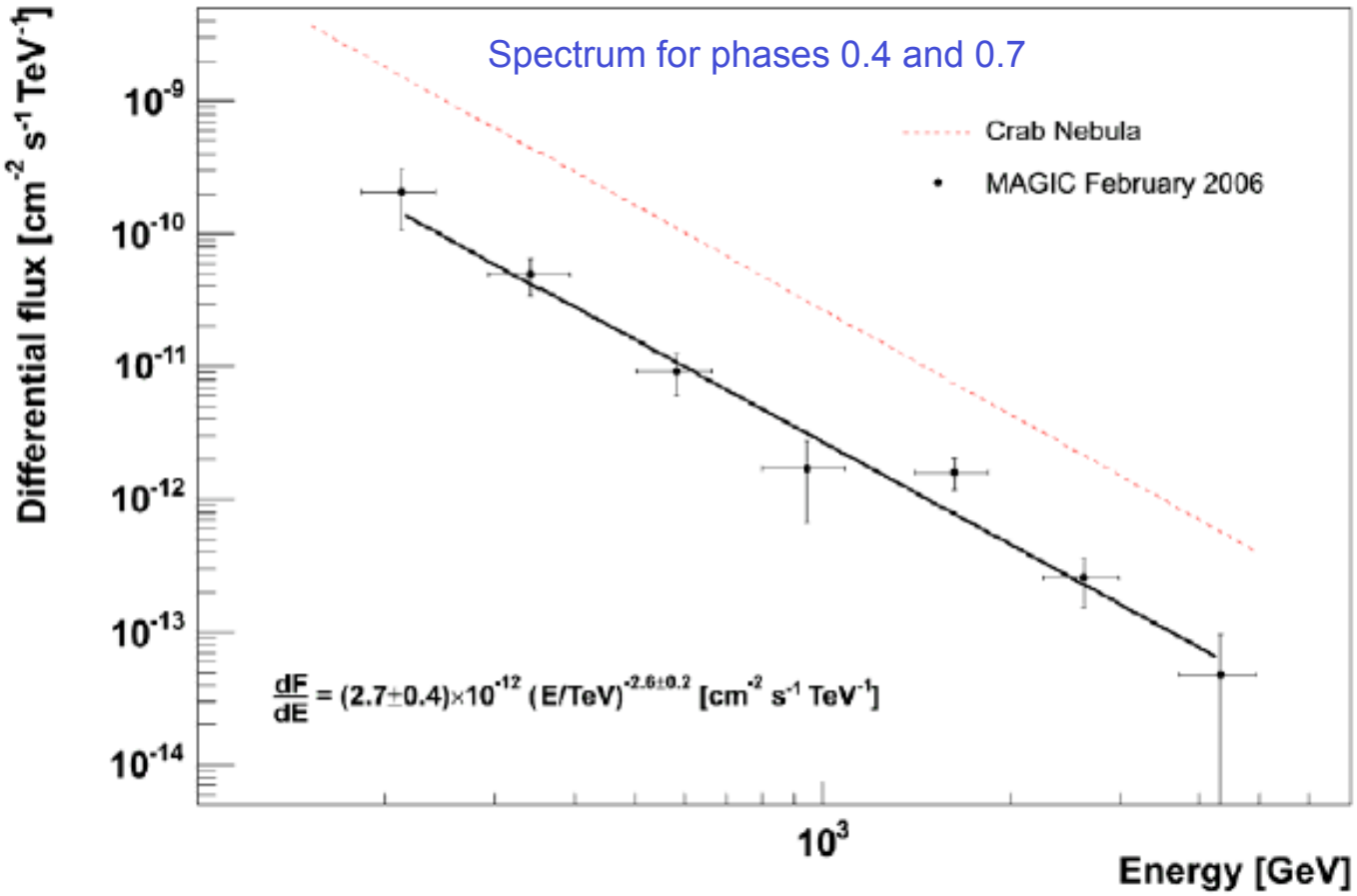

This spectrum is consistent with that of EGRET for a spectral break between 10 and 100 GeV. We estimate that the flux from LS I +61 303 above 200 GeV corresponds to an isotropic luminosity of ~7 x 10^{33} erg s^{-1}, at a distance of 2 kpc. The intrinsic luminosity of LS I +61 303 at its maximum is a factor ~6 higher than that of LS 5039, and a factor ~2 lower than the combined upper limit (<8.8 x 10^{-12} cm^{-2} s^{-1} above 500 GeV) obtained by Whipple (Fegan et al. 2005, ApJ 624, 638).

Radio 15 GHz /Ryle, simultaneous with MAGIC obs.

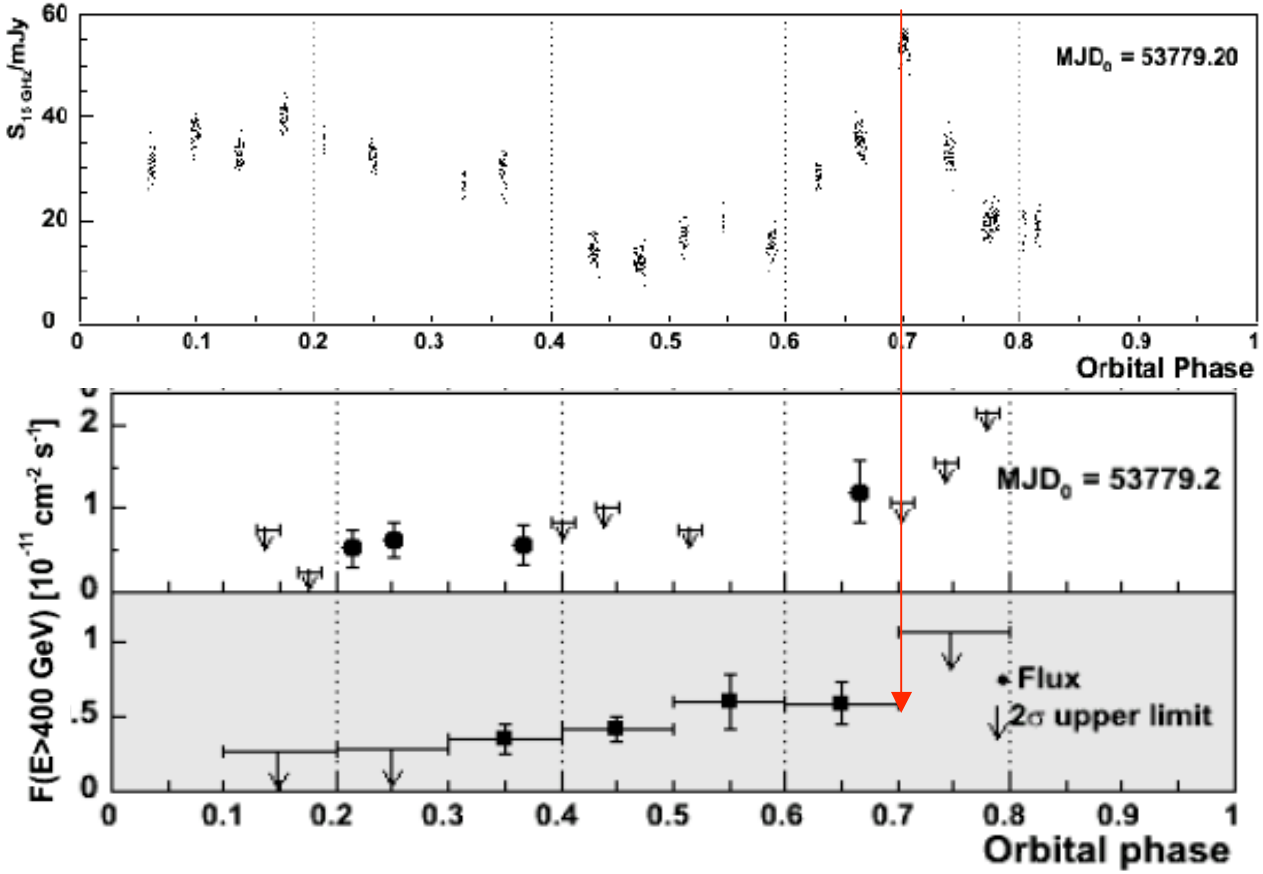

The TeV flux maximum is detected at phases 0.5-0.6, overlapping with the X-ray outburst and the onset of the radio outburst. The maximum flux is not detected at periastron, when the accretion rate is expected to be the largest (Martí&Paredes 1995, A&A 298, 151). This result seems to favor the leptonic over the hadronic models, since the IC efficiency is likely to be higher than that of proton-proton collisions at the relatively large distances from the companion star at this orbital phase.

Concerning energetics, a relativistic power of several 10^{35} erg s^{-1} could explain the non thermal luminosity of the source from radio to VHE gamma-rays. This power can be extracted from accretion in a slow inhomogeneous wind along the orbit (Bednarek 2006, MNRAS 268, 579).

The variable nature of the TeV emission on timescales of ~1 day constrains the emitting region to be smaller than a few 10^{15} cm (or ~0.1 arcsec at 2 kpc). This is compatible with the emission being produced within the binary system, where there are large densities of seed photons for IC interaction. Under these strong photon fields opacity effects certainly play a role in the modulation of the emitted radiation (Dubus 2006, A&A 451, 9).

Propagation of very high energy gamma-rays inside massive binaries LS 5039 and LSI +61 303

Bednarek 2006, MNRAS 268, 579

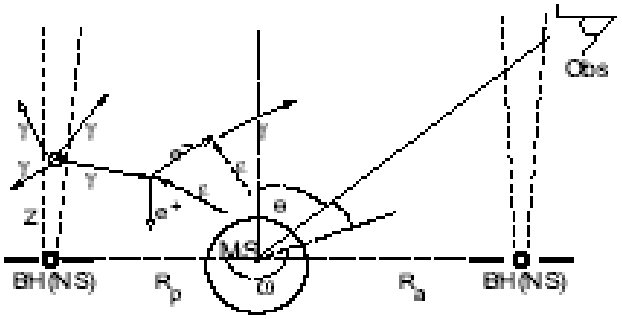

Figure 1. Schematic picture of a compact binary system composed of a massive star and a compact object (a black hole or an neutron star) on an orbit around the massive OB star. The observer is located at the inclination angle _ and the azimuthal angle _. The matter accreting onto a compact object from the massive star creates an accretion disk. Particles (electrons or protons) are accelerated inside the jet launched from the inner part of an accretion disk. Primary electrons and/or gamma-rays, injected at the distance z from the base of the jet, initiate an anisotropic inverse Compton e± pair cascade in the radiation field of the massive star. A part of the primary gamma-rays and secondary cascade gamma-rays escape from the binary system toward the observer.

The cascade processes occurring inside these binary systems significantly reduce the gamma-ray opacity obtained in other works by simple calculations of the escape of gamma-rays from the radiation fields of the massive stars

The maximum in TeV gamma-ray light curve predicted by the propagation effects in LSI +61 303 should occur after periastron passage (as has been observed).

Interaction of the relativistic wind from a young pulsar with the wind from its stellar companion

Dubus 2006, A&A in press (astro-ph/0605287)

LSI +61 303

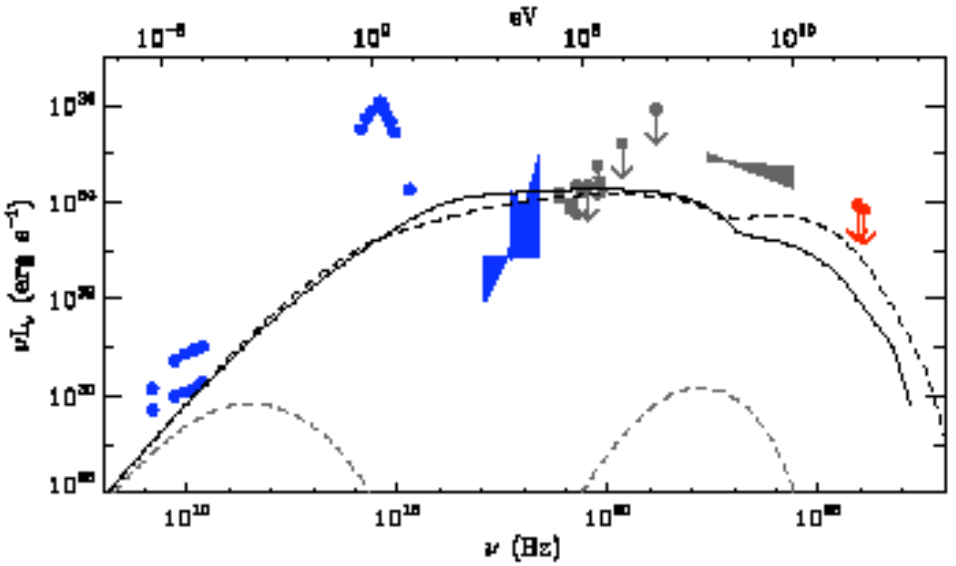

Stellar wind is equatorial
Periastron: full black lines
Apastron: dashed black lines

A model based on accretion of matter from the slow inhomogeneous equatorial wind of the primary star

Bosch-Ramon et al. 2006,
A&A in preparation

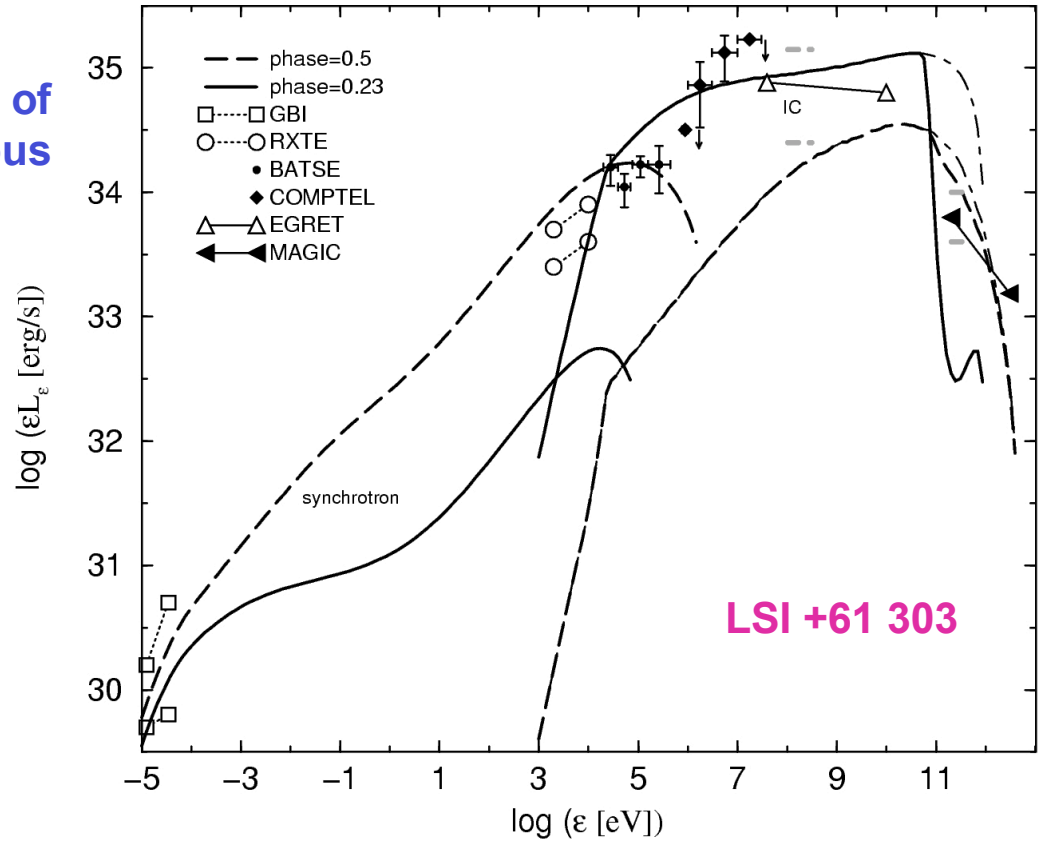

- Particle injection proportional to the accretion rate
- Relativistic electron energy distribution is computed taking into account convective/adiabatical and radiative losses
- SED computed taking into account synchrotron and (Thomson/Klein Nishina) IC, and the photon-photon absorption in the ambient photon fields
- The geometry of the photon-photon and the electron-photon interaction, which changes along the orbit, is considered in the calculations of the gamma-ray opacity and IC emission.

Summary

- Microquasars mimic also the quasars as HE and VHE emitters
- Microquasars are among the most interesting sources in the galaxy from the viewpoint of high-energy astrophysics.
- Models predict that radio jets could be natural sites for the production of high energy photons via both Compton scattering and maybe direct synchrotron emission.
- From the analogy with quasars, microquasars should be (and are) _-ray emitters.
- Up to now, above ~ 500 keV, a handful of μqs have been detected:
  Cygnus X-1 at ≥ 1 MeV, GRO J1655-40 at ~1 MeV,
  GRS 1915+105 and Cygnus X-3 at TeV?
  LS 5039 and LSI+61303: 100 MeV - few TeV
- More microquasars will be detected soon with the Cherenkov telescopes and GLAST. This will bring more constraints to the physics of these systems and its relation with AGNs.

FAST PRECESSION… in only 24 hours !

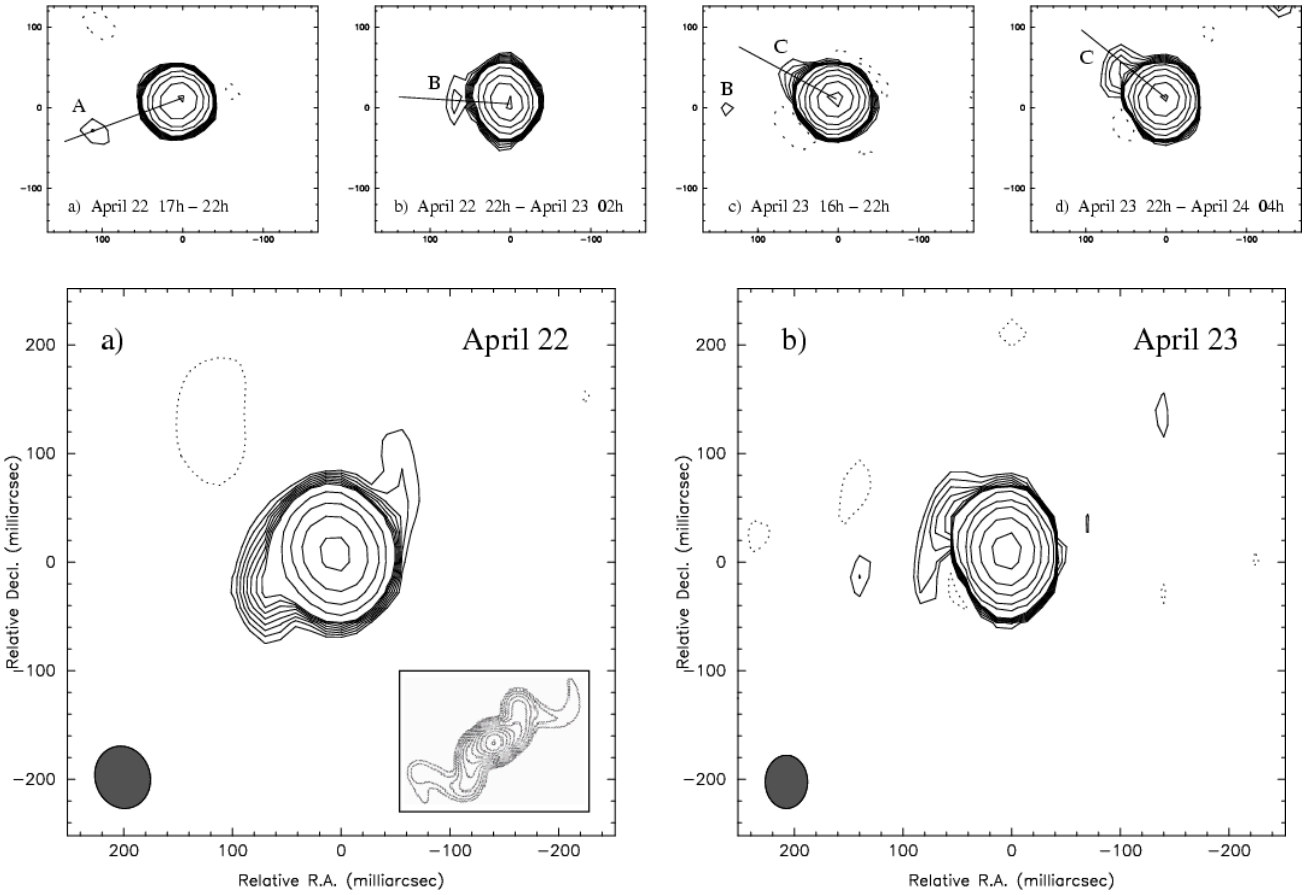

LS I+61 303 (MERLIN at 5 GHz)

Massi et al. 2004, A&A 414, L1

Precession could explain:

- the puzzling VLBI structures observed so far

Radial velocity curve of LSI+61303

Casares et al. 2005, MNRAS, 360, 1105

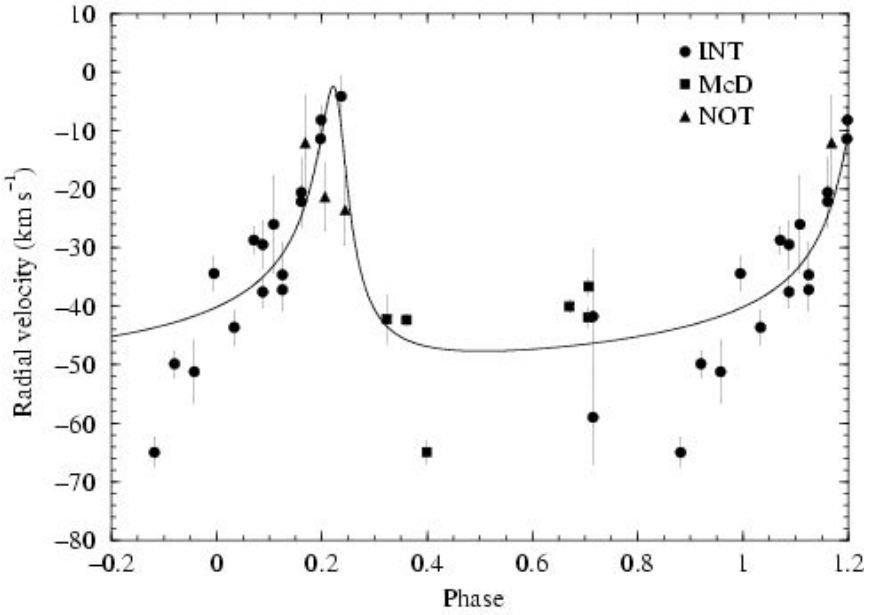

New orbital ephemeris!!

e = 0.72 ± 0.15
_ = 21.0 ± 12.7 º
v = - 40.2 ± 1.9 km/s
K1 = 22.6 ± 6.3 km/s
a_1 sin i = 8.2 ± 2.9 R$_\odot$
f(m) = 0.0107$_{-0.0077}^{+0.0163}$M$_\odot$

Periastron at orbital phase of 0.23

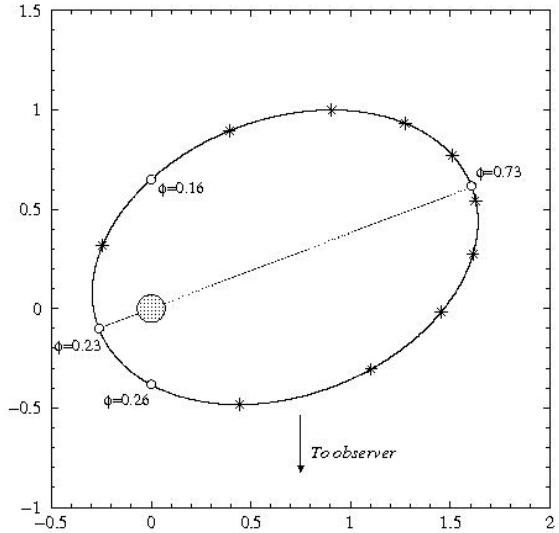

BH for i ≤ 25º
NS for 25º ≤ i ≤ 60º
~~WD for i ≥ 60°~~

v sin i = 113 km/s

i ~ 30 ± 20º

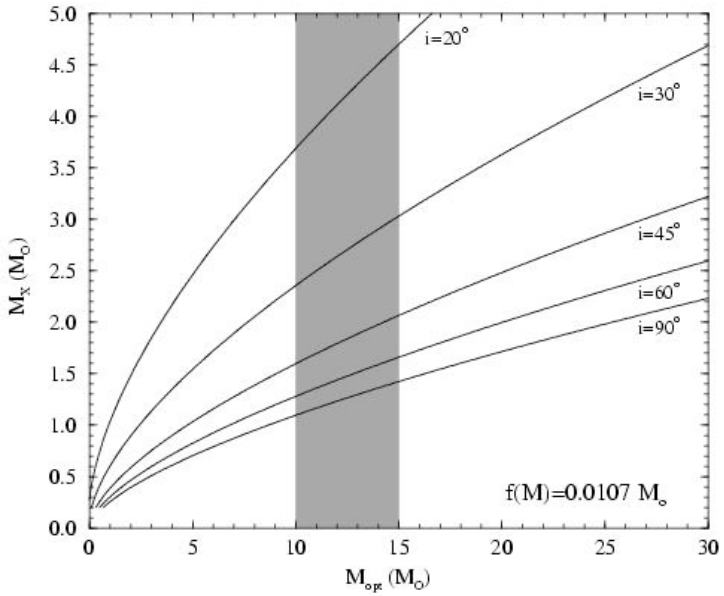

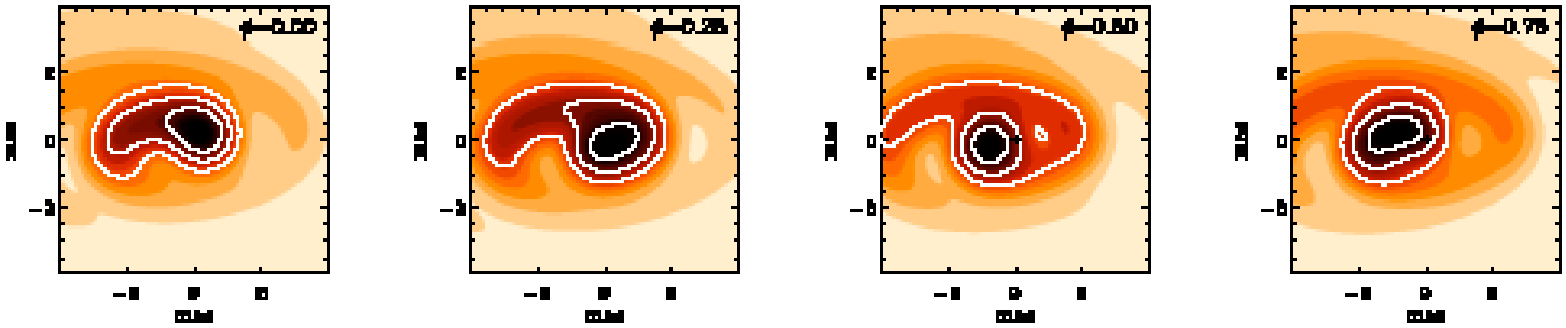

Fig. 7. Orbital evolution of the 5 GHz radio emission from the pulsar nebula in LS 5039. The maps were composed by summing up the contributions along the spiral nebula, as calculated for the various orbital phases ϕ (see Fig. 5 for the ϕ=0 case). The maps were then smoothed by a gaussian kernel with a Full-Width at Half Maximum (FWHM) of 0.8 mas ($3\ 10^{12}$ cm at 2.5 kpc). The maps share a common color scale to allow direct comparison, with contours at 50%, 25% and 10% of the maximum orbital radio emission. The maps at ϕ=0-0.25 are very similar to that observed by Paredes et al. (2000).

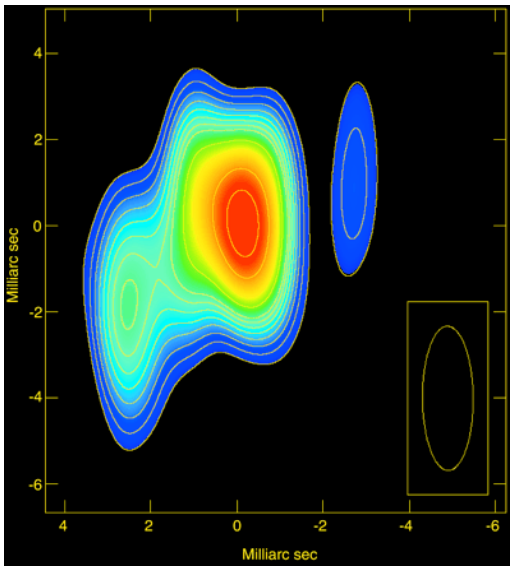

VLBA, phase 0.2

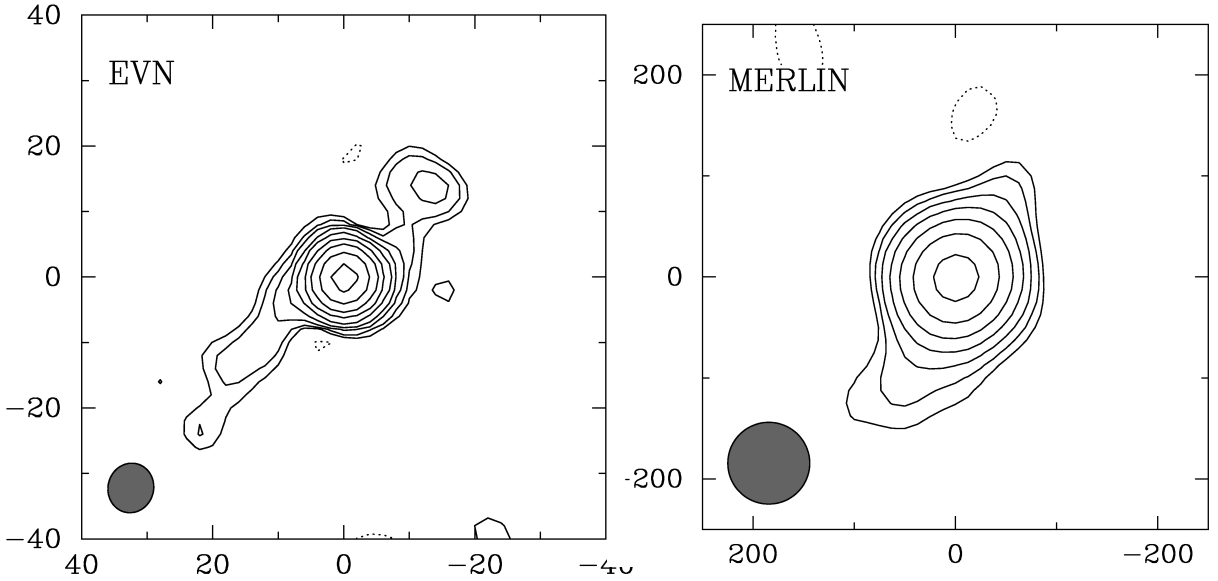

phase 0.5

25 jets detected in X-rays in AGNs, most of them radio-galaxies (both FRI and FRII)

SSC model cannot explain the level of X-ray emission

The mechanism responsible is the IC scattering of seed photons of both, the CMB radiation and the nucleus, by relativistic electrons in the jet
Tavecchio et al. 2000, ApJ 544, L23; Celotti et al. 2001, MNRAS 321, L1

Powerful FRII jets in QSO should be good candidate for high-energy emission

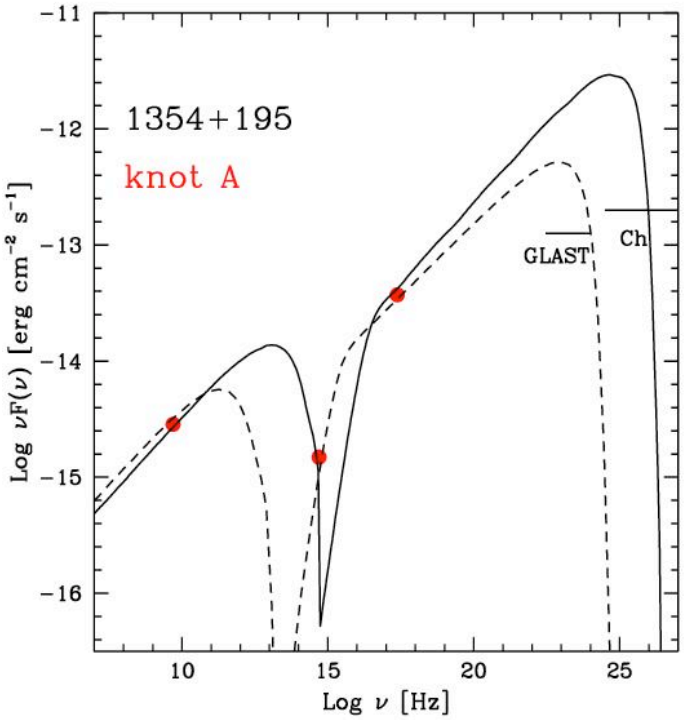

Sambruna et al. 2002, ApJ 571, 206
Tavecchio 2004, astro-ph 0401590

___ : the optical is synch.
----- : IC/CMB

RXTE observations of LS5039 covering a full orbital period

- An increase of emission around periastron passage, as expected in an accretion scenario
- Changes in the photon index, anticorrelated with flux variations
- Simultaneous INT: Constant EW of the H_ absorption line no significant changes of the mass-loss rate of the primary

- The variability is due to changes of the accretion rate in an eccentric orbit
- X-ray radiation produced by IC processes in the jet of the microquasar

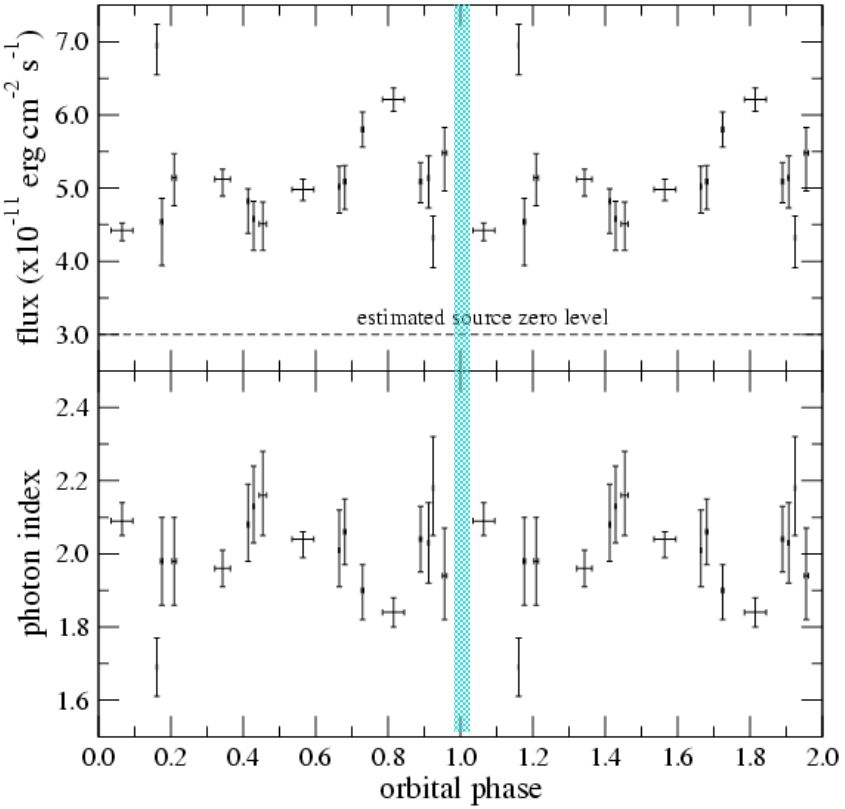

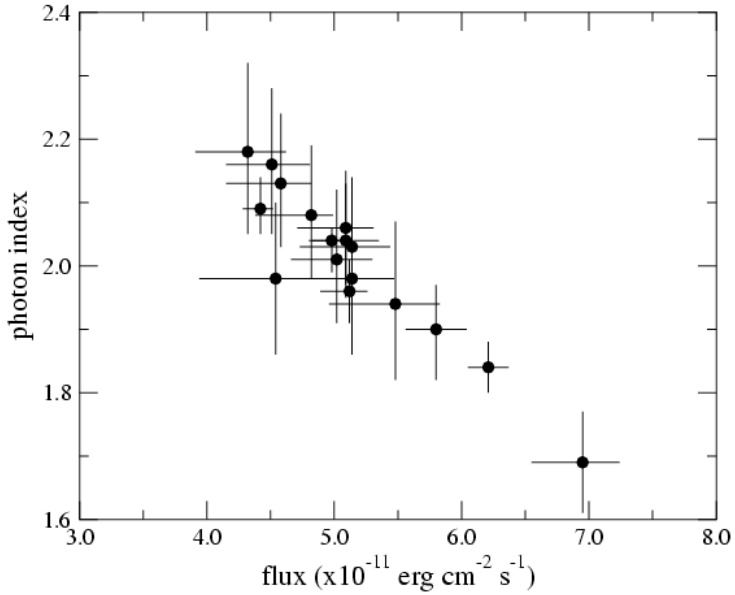

RXTE (3 – 30 keV), 4 – 8 July 2003

Bosch-Ramon, Paredes, Ribó et al., 2005, ApJ, in press

Model for the _-ray emission of LSI+61303

EGRET+Whipple data

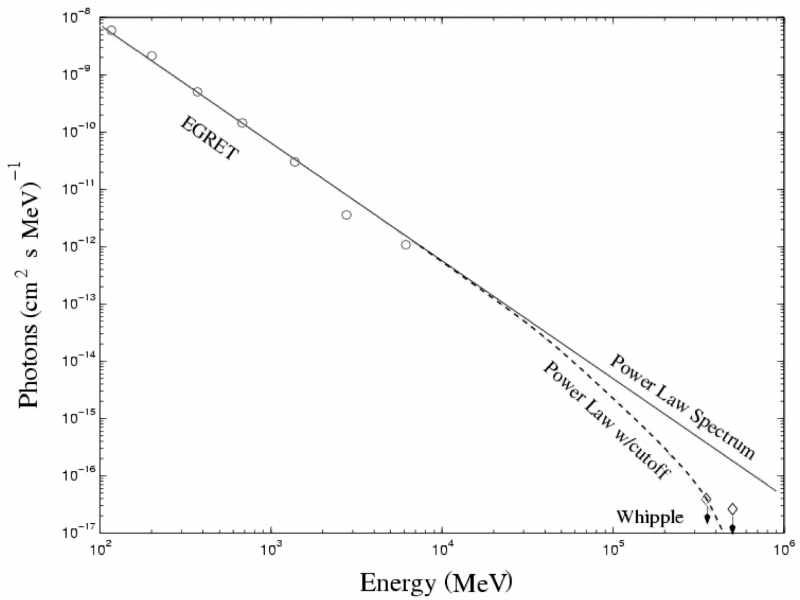

TABLE 1

RESULTS OF THE SEARCH FOR STEADY, UNPULSED, HIGH-ENERGY EMISSION FROM LS I +61°303

Data Set	Exposure (minutes)	Significance (σ)	Flux Upper Limit ($\times 10^{-11}$ cm^{-2} s^{-1})
1994–1996	1397.5	1.39	$\leq 0.92^{a}$
1998	424.7	1.50	$\leq 1.23^{b}$
Combined data sets ...	1822.2	0.78	$\leq 0.88^{b}$

[a] Energy threshold of 350 GeV.
[b] Energy threshold of 500 GeV.

Hall et al. 2003, ApJ 583, 853

Synchrotron, IC and SSC losses have been taken into account.

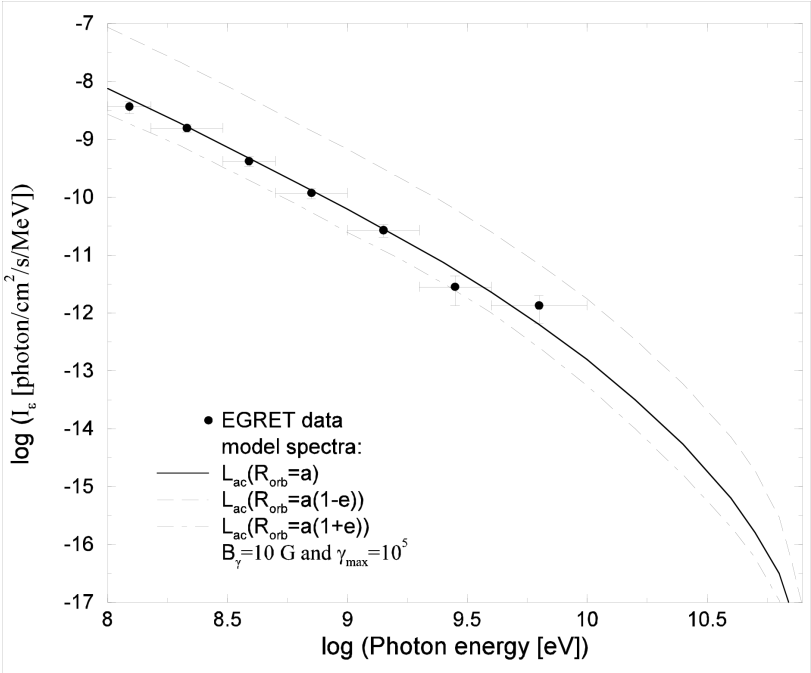

Bosch-Ramon & Paredes 2004, A&A, in press

- If the relativistic electrons of the jet reach energies of about 1 TeV, then the IC mechanism can produce detectable emission at 100 GeV.

Models for SSC emission - LMXB

•Jet exposed to star, disk and corona photon fields.

Applied to LMXB (Grenier, Kaufman Bernadó & Romero, Ap&SS, astro-ph/0408215)

- In contrast with high-mass systems where the external radiation energy density largely surpasses the magnetic one, SSC emission is likely to dominate even for a modest field strength of _ 10 G in the jet
- _ _ absorption against the disc photons is not included although it efficiently limits the emerging _-ray flux. Adiabatic losses in an expanding jet would also modify the result although not severely.

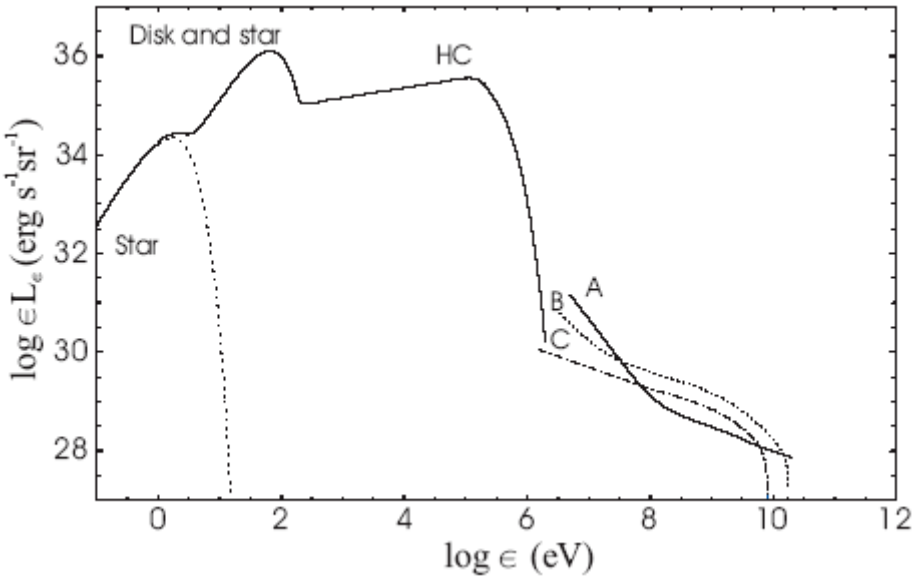

- Very low luminosities are predicted

Spectral energy distribution of the EC emission from the jet of a microquasar with an F star companion, seen at angles of 5° (A), 15° (B), and 30° (C) from its axis, for $\_{jet}$ =3, q_{jet}=1% and $E^{-2.3}$ pair spectrum between 1 MeV and 5 GeV.

Similarities between these EGRET candidates

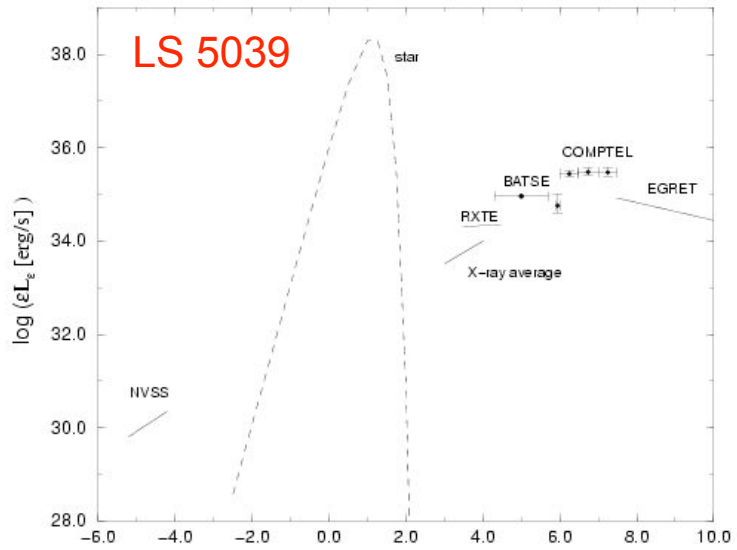

Bosch-Ramon et al. 2004, A&A, submitted

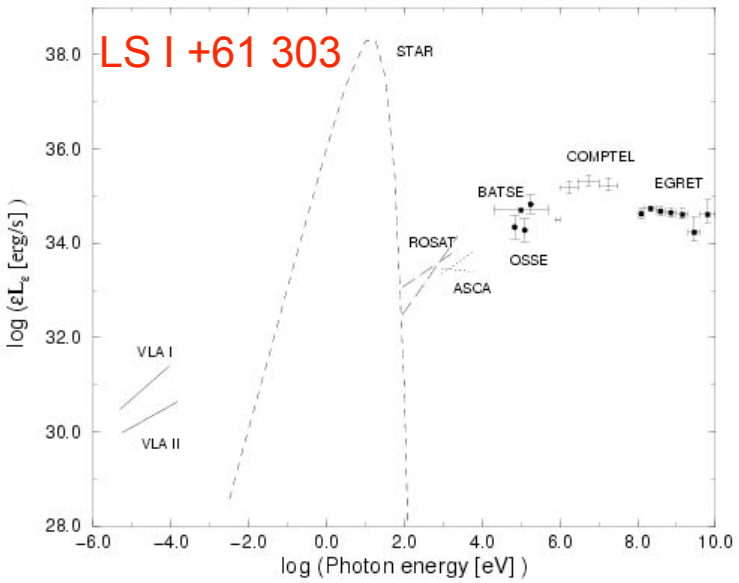

Semi-analytical approach
Parametrization of the energy evolution

Maximum electron Lorentz factor $\gamma_{e\,max} \sim 10^4$

Kinetic luminosity or jet power $L_k \sim 10^{36}$ erg/s

Inner-jet radius $R_{jet} \sim 10^7$ cm

Electron energy distribution power-law index $p_e = 2$

Jet Lorentz factor $\gamma_{jet} = 1.1$

Angle between the jet and the observer line of sight $\theta_{obs} = 10^o$

Star luminosity $L_{star} \sim 5x10^{39}$ erg/s

Disc luminosity $L_{disc} \sim 3x10^{32}$ erg/s

Corona luminosity $L_{cor} \sim 3x10^{32}$ erg/s